

NATIONAL ADVISORY COMMITTEE FOR AERONAUTICS

WARTIME REPORT

ORIGINALLY ISSUED
May 1944 as
Advance Confidential Report L4E01

ANALYSIS OF AVAILABLE DATA ON THE EFFECTIVENESS OF
AILERONS WITHOUT EXPOSED OVERHANG BALANCE

By Robert S. Swanson and Stewart M. Crandall

Langley Memorial Aeronautical Laboratory
Langley Field, Va.

The NACA logo features the word "NACA" in a bold, sans-serif font, centered within a stylized wing shape that tapers at the ends.

WASHINGTON

NACA WARTIME REPORTS are reprints of papers originally issued to provide rapid distribution of advance research results to an authorized group requiring them for the war effort. They were previously held under a security status but are now unclassified. Some of these reports were not technically edited. All have been reproduced without change in order to expedite general distribution.

Digitized by the Internet Archive
in 2011 with funding from
University of Florida, George A. Smathers Libraries with support from LYRASIS and the Sloan Foundation

NATIONAL ADVISORY COMMITTEE FOR AERONAUTICS

ADVANCE CONFIDENTIAL REPORT

ANALYSIS OF AVAILABLE DATA ON THE EFFECTIVENESS OF
AILERONS WITHOUT EXPOSED OVERHANG BALANCE

By Robert S. Swanson and Stewart M. Crandall

SUMMARY

A considerable amount of two- and three-dimensional data on the effectiveness of ailerons without exposed overhang balance has been collected and analyzed. The trends indicated by the analysis have been summarized in the form of a few approximate rules concerning the effectiveness parameter $\Delta\alpha/\Delta\delta$ (at constant lift): Thickening and beveling the trailing edge (as measured by the trailing-edge angle θ) will generally reduce the effectiveness about 0.3 percent per degree of bevel for ailerons sealed at the hinge axis and about 0.6 percent per degree of bevel for unsealed ailerons. A 0.005c gap at the hinge axis usually reduces the effectiveness approximately 17 percent for flap chord ratios of 0.2. This percentage increases as the flap chord ratio is reduced. The effectiveness is about 14 percent lower at aileron deflections of 20° than at aileron deflections of 10° . At large angles of attack ($\alpha = 10^\circ$) and for chord ratios of about 0.2, positively deflected ailerons are approximately 20 percent less effective than negatively deflected ailerons. The deflection of partial-span flaps has no consistent effect on the effectiveness. Increases in Mach number and forward movement of the transition point decrease the aileron effectiveness.

No consistent deviation of the experimentally determined values of static rolling moments from those values predicted by the lifting-line-theory method could be detected. Because the several factors neglected in the lifting-line theory apparently are fairly small and counteract one another, on the average, no additional correction need be applied.

INTRODUCTION

As a part of the general lateral-control investigation by the NACA, the large amount of two- and three-dimensional data on the rolling effectiveness of ailerons without exposed overhang balance is collected and analyzed in the present paper. The main purpose of the analysis is to determine any fairly consistent variations in the effectiveness of these ailerons with the various design variables and criteria of similitude.

The secondary purpose of the analysis is to evaluate experimentally the limitations of lifting-line theory with regard to the estimation of aileron rolling moments from section data.

SYMBOLS

C_L	wing lift coefficient
$C_{L_{max}}$	maximum wing lift coefficient
c_l	section lift coefficient
C_l	wing rolling-moment coefficient
α	angle of attack, degrees
δ	flap or aileron deflection, degrees
b	wing span
y	spanwise location
y_o	spanwise location of outboard end of aileron
y_i	spanwise location of inboard end of aileron
S	wing area
A	aspect ratio (b^2/S)
λ	taper ratio, that is, fictitious chord at tip divided by chord at root

- c wing chord at any section
- c_f flap chord at any section
- c_a aileron chord at any section
- ϕ airfoil trailing-edge angle, degrees
- M Mach number, ratio of free-stream velocity to velocity of sound
- R Reynolds number
- a_0 slope of curve of section lift coefficient against angle of attack at constant δ

$$\left[(\partial c_L / \partial \alpha)_\delta \right]$$
- $(\partial c_L / \partial \delta)_\alpha$ slope of curve of section lift coefficient against flap deflection at constant α
- $\Delta \alpha / \Delta \delta$ section flap effectiveness parameter, that is, absolute value of ratio of equivalent change in angle of attack to angle of flap deflection measured at constant lift
- $(\Delta \alpha / \Delta \delta)_3$ aileron effectiveness parameter, that is, ratio of equivalent change of angle of attack to angle of aileron deflection; subscript 3 indicates that values are computed from three-dimensional test data by use of lifting-line theory
- K theoretical or experimental correction to lifting-line-theory values of rolling moment

$$\left[\frac{(\Delta \alpha / \Delta \delta)_3}{\Delta \alpha / \Delta \delta} \right]$$
- τ wind-tunnel turbulence factor

Subscript $\delta = 0^\circ$ to $\pm 10^\circ$, $\delta = 0^\circ$ to $\pm 15^\circ$, or $\delta = 0^\circ$ to $\pm 20^\circ$, etc., indicates range over which $\Delta \alpha / \Delta \delta$ or $(\Delta \alpha / \Delta \delta)_3$ is evaluated.

DATA

Scope

The characteristics of the two- and three-dimensional models and the air-flow characteristics of the wind tunnels in which the models were tested are summarized in tables I and II, respectively. The data as given in the original reports (references 1 to 24) were in many cases uncorrected for the effects of the jet boundaries or for model deflections. It was found essential to apply such corrections before the data could be correlated.

Reduction and Presentation of Data

Section data.- The effectiveness parameter $\Delta\alpha/\Delta\delta$ is the section characteristic of flaps that determines their ability to provide rolling motion when installed as ailerons on an airplane, provided the analysis is based on aileron deflection rather than stick force. This parameter $\Delta\alpha/\Delta\delta$ is equal to the absolute value of the change in angle of attack necessary to neutralize the lift produced by a unit flap deflection. The effectiveness parameter was determined from the section data of references 1 to 15 by plotting α against δ for a constant section lift coefficient c_l and measuring the slope (absolute value of slope used) of a straight line through $\delta = 0^\circ$ and $\delta = 10^\circ$ for the effectiveness at small flap deflections $(\Delta\alpha/\Delta\delta)_{\delta=0^\circ \text{ to } 10^\circ}$ and through $\delta = 0^\circ$ and $\delta = 20^\circ$ for the effectiveness at large flap deflections $(\Delta\alpha/\Delta\delta)_{\delta=0^\circ \text{ to } 20^\circ}$. It is often convenient in the analysis to consider the limiting case of $\partial\alpha/\partial\delta$, which is equivalent to $\frac{(\partial c_l / \partial \delta)_\alpha}{(\partial c_l / \partial \alpha)_\delta}$. For practical purposes, the values of $(\Delta\alpha/\Delta\delta)_{\delta=0^\circ \text{ to } 10^\circ}$ are very nearly equal to the values of $\partial\alpha/\partial\delta$.

Static three-dimensional data.- In references 25 and 26 are presented charts for estimating the rolling moment caused by aileron deflection. The charts were calculated from lifting-line theory for various wing and aileron plan forms for a slope of the section lift curve of 0.099 per degree. The general method for using the

charts to determine the rolling-moment coefficient C_L is to evaluate graphically the following integral across the aileron span:

$$C_L = \delta \frac{a_0}{0.099} K \int \frac{\Delta \alpha}{\Delta \delta} \frac{d \frac{C_L}{\alpha}}{d \frac{y}{b/2}} d \frac{y}{b/2} \quad (1a)$$

or

$$C_L = \delta \frac{a_0}{0.099} K \int \frac{\Delta \alpha}{\Delta \delta} d \frac{C_L}{\alpha} \quad (1b)$$

where

- a_0 slope of section lift curve, per degree
 K experimental or theoretical correction to lifting-line theory (to be evaluated)
 $\Delta \alpha / \Delta \delta$ experimental section lift effectiveness of aileron

C_L / α is determined from the charts of reference 25 or 26, and y is measured along the wing span. If $\Delta \alpha / \Delta \delta$ is constant across the aileron, the integral is equal to $\Delta \alpha / \Delta \delta$ times the difference between the end values of C_L / α .

Most of the models studied had ailerons of constant chord ratio and $\Delta \alpha / \Delta \delta$ thus was a constant. By inserting experimental values of C_L and chart values

of C_L / α in equation (1a), $\frac{a_0}{0.099} \left(\frac{\Delta \alpha}{\Delta \delta} \right)_3$ or its equivalent $\frac{a_0}{0.099} K \frac{\Delta \alpha}{\Delta \delta}$ therefore could be evaluated. A few

erroneous values in references 25 and 26 were corrected and the curves were refaired to be similar to the known fairing for elliptical wings. By using section data to estimate a_0 and $\Delta \alpha / \Delta \delta$, the value of K could be experimentally evaluated. If section data for evaluating a_0 were not available, a_0 was estimated by using the measured slope for the finite-span wing in the lifting-line-theory formulas (reference 27) corrected for

the edge velocity by the methods of reference 28. For these cases in which a_0 could not be satisfactorily

estimated, the data are presented as $\frac{a_0}{0.099} \left(\frac{\Delta\alpha}{\Delta\delta} \right)_3$.

For the few cases in which the aileron chord ratio was not constant across the aileron span, the integral of equation (1a) was evaluated by using the section data of figure 1 to estimate the variation of $\Delta\alpha/\Delta\delta$ with c_a/c ; thus an effective average value of c_a/c , weighted according to the ability of each spanwise aileron section to produce rolling moment, was evaluated.

DISCUSSION

Effect of Viscosity

From figures 1 and 2, the effectiveness $\Delta\alpha/\Delta\delta$ of sealed plain flaps and ailerons with small trailing-edge angles is seen to be considerably less than the theoretical values for thin airfoils. Most of the decrease in effectiveness may be attributed to the influence of viscosity. The effective surface or boundary of the airfoil is displaced from the actual surface by the amount of the so-called displacement thickness, which is the height of the mean ordinate of the velocity distribution in the boundary layer. Because the shapes and thicknesses of boundary layers vary with pressure gradient, transition location, Reynolds number, Mach number, gap at hinge axis, etc., the effective airfoil shape varies with these factors.

The flap effectiveness $\Delta\alpha/\Delta\delta$ is less than the theoretical value because the rate of increase of the thickness of the boundary layer with flap deflection, which results from the high adverse pressure gradient behind the hinge axis, is usually greater than the rate of increase of the boundary-layer thickness with angle of attack. The slope $(\partial c_l / \partial \delta)_\alpha$ is therefore decreased more by viscosity than is $(\partial c_l / \partial \alpha)_\delta$; $\Delta\alpha/\Delta\delta$ is thus decreased by viscosity. The larger the flap deflection, the smaller the effectiveness $\Delta\alpha/\Delta\delta$. The section data of figure 3 and the finite-span data of figure 4 show

that, at low angles of attack, the effectiveness at flap deflections of 20° is approximately 14 percent lower than the effectiveness at flap deflections of 10° . At high angles of attack, approximately the same reduction occurs (fig. 5), except for the gap-unsealed condition in which little consistent reduction is in evidence.

The effect of viscosity upon the aileron effectiveness depends markedly upon the pressure gradient. The direction of the deflection of an aileron would be expected to have little effect at small angles of attack because the pressure distribution at $\delta = 0^\circ$ is very nearly the same on both surfaces. The data of figure 6 verify this deduction. At high angles of attack, however, negative aileron deflections reduce the adverse pressure gradient whereas positive aileron deflections increase the adverse pressure gradient. A lower effectiveness thus may be expected for positive aileron deflections. The data of figure 7 indicate that, at an angle of attack of 10° and for chord ratios of about 0.2, positively deflected ailerons are about 20 percent less effective than negatively deflected ailerons. This effect appears to increase with aileron chord ratio.

The gap at the flap hinge axis allows the low-energy boundary-layer air to leak from the pressure side to the suction side of the airfoil. The boundary layer on the pressure side is thus thinned and on the suction side is further thickened with a resulting reduction of the lift increment. The effect of the gap on the lift-curve slope due to angle of attack $(\partial c_l / \partial \alpha)_\delta$ is fairly small, because the pressure difference across the hinge axis is small. The slope $(\partial c_l / \partial \delta)_\alpha$, and consequently $\Delta \alpha / \Delta \delta$, is considerably decreased, however, because the maximum pressure difference due to flap deflection is usually located at the hinge axis. Figure 8 shows that a 0.005c gap at the hinge axis decreases the effectiveness about 17 percent for flap chord ratios of 0.2. This reduction appears to be larger for flaps of smaller chord.

A forward movement of the transition point usually increases the thickness of the boundary layer and thus decreases the flap effectiveness $\Delta \alpha / \Delta \delta$. This effect is shown qualitatively in figure 9, in which data are presented from tests with and without the nose of the airfoil roughened in order to fix transition. The position

of the transition point on the unroughened airfoil was not determined. Some unpublished computations and experimental data indicate that a reduction of about 2 percent in $\Delta\alpha/\Delta\delta$ for a forward transition movement of 0.1c may be expected with sealed plain flaps. The effects of viscosity are usually greater with increased thickness and beveling of the airfoil trailing edge. The effect of transition movements and gaps thus are greater for airfoils with large trailing-edge angles ϕ . Gaps at the aileron hinge axis also increase the loss in $\Delta\alpha/\Delta\delta$ that results from transition movements.

The effect of beveling the trailing edge of the flap is presented in figure 9, in which the effectiveness $(\Delta\alpha/\Delta\delta)_{\delta=0 \text{ to } 10^\circ}$ is shown as a function of the trailing-edge angle ϕ . Reductions of about 0.4 percent per degree of bevel for sealed flaps and of about 1 percent per degree of bevel for unsealed flaps are indicated. The three-dimensional data of figure 10 show a decrease in aileron effectiveness of about 0.3 percent per degree of bevel for sealed ailerons and approximately 0.6 percent per degree of bevel for unsealed ailerons.

It should be noted that, under some particular conditions, viscosity may increase $\Delta\alpha/\Delta\delta$ to values even greater than those for the theoretical thin airfoil. The explanation for this rather astonishing fact is quite simple. The effectiveness parameter $\Delta\alpha/\Delta\delta$ is equal to the ratio of the lift-curve slopes $\frac{(\partial c_l / \partial \delta)_\alpha}{(\partial c_l / \partial \alpha)_\delta}$. If viscosity decreases $(\partial c_l / \partial \alpha)_\delta$ more than it decreases $(\partial c_l / \partial \delta)_\alpha$, the effectiveness parameter $\Delta\alpha/\Delta\delta$ is increased. For a few conditions, markedly low lift-curve slopes $(\partial c_l / \partial \alpha)_\delta$ occur over a small range of angle of attack α . Also, the slope $(\partial c_l / \partial \delta)_\alpha$ is less affected or is affected over a different range of α . Over a limited range of α , very large values of $\Delta\alpha/\Delta\delta$ may therefore occur. A few cases in which this phenomenon has been observed are: (1) negatively deflected ailerons at large angles of attack near the stall, (2) so-called linked-balance ailerons with which a gap through the wing occurs well ahead of the hinge axis and allows very low values of $(\partial c_l / \partial \alpha)_\delta$ but has little effect on $(\partial c_l / \partial \delta)_\alpha$.

near $\alpha = 0^\circ$, and (3) ailerons on low-drag airfoils with large trailing-edge angles, which usually have a very large value of effectiveness $\Delta\alpha/\Delta\delta$ near the angles of attack where the transition point suddenly shifts forward (near boundary of low-drag region) and causes a break in the curve of c_l against α .

Effect of Compressibility

Data on the effect of Mach number on $(\Delta\alpha/\Delta\delta)_{\delta} = -10^\circ$ to 10° are shown in figure 11. The data are rather limited and subject to some doubt because it is extremely difficult to determine accurately the wind-tunnel corrections at large values of Mach number. Corrections for model twist and deflections were applied to the data. Increasing the Mach number usually decreases $\Delta\alpha/\Delta\delta$. From figure 11, it may be seen that an increase in Mach number from 0.2 to 0.45 reduces the effectiveness about 7 percent.

The simple theory of Glauert and Prandtl indicates no effect of Mach number on $\Delta\alpha/\Delta\delta$ because $(\partial c_l/\partial \alpha)_{\delta}$ and $(\partial c_l/\partial \delta)_{\alpha}$ are assumed to be increased equally by compressibility. Experimental data indicate, however, that $(\partial c_l/\partial \alpha)_{\delta}$ is usually increased a little more and $(\partial c_l/\partial \delta)_{\alpha}$ a little less than the Glauert-Prandtl relation would account for. The explanation appears to be related to the thickening of the boundary layer and the transition changes that have been observed at high Mach numbers. It is believed, therefore, that below the critical speed the main effect of compressibility upon $\Delta\alpha/\Delta\delta$ is to increase the effects of viscosity.

Corrections to Lifting-Line Theory

The limitations of lifting-line theory for the estimation of aileron hinge-moment characteristics from section data were discussed in reference 28. The aspect-ratio corrections to the hinge moment determined from lifting-line theory were shown to be inadequate whereas, for the cases in which lifting-surface-theory calculations (reference 28) are available, the aspect-ratio corrections to the hinge moment determined from lifting-surface theory are shown to be satisfactory. The large

difference between the results of the two theories may be illustrated by the fact that the aspect-ratio corrections to the slope of the curve of hinge moment against angle of attack determined from lifting-surface theory are about twice as great as the corrections determined from lifting-line theory.

The aspect-ratio corrections to the slope of the lift curve against angle of attack (references 29 and 30) for moderate aspect ratio as determined by the lifting-line and lifting-surface theories differ by only about 7 or 8 percent. The aspect-ratio corrections to the damping moments of elliptical wings rotating about the lateral plane of symmetry as determined by the two theories also differ by only about 7 or 8 percent (unpublished correction determined by the methods of reference 30). The difference between the two aspect-ratio corrections to the slope of the lift curve against flap deflection is about 3 to 4 percent, which is only about one-half as much as that for the slope of the lift curve against angle of attack. This difference exists primarily because the distance to the three-quarter-chord point (point for best measure of effective angle of attack of wing) from the center of load that results from aileron deflection is roughly one-half the distance to the three-quarter-chord point from the center of load that results from changes in angle of attack. The effective length of the trailing vortices thus is less for the load that results from flap deflection. It might therefore be expected that the aspect-ratio correction to the static aileron rolling moments determined from lifting-surface theory would be of the same order, 3 to 4 percent greater than the value determined from lifting-line theory. In any case, the aileron rolling moments determined from lifting-line theory should be much closer to the experimental values than the aileron hinge moments would be.

It may be seen that the section data (fig. 1) and the finite-span data with the lifting-line-theory aspect-ratio corrections applied (fig. 2) are in fairly good agreement. Although there is considerable scatter, the curve faired through the section data represents very well the finite-span data, especially for aileron chord ratios of 0.2 or less. (See fig. 2.) An experimental evaluation of the over-all aspect-ratio corrections shows, on the average, no serious discrepancies (exceeding 10 percent) with the lifting-line-theory values; that is,

on the average, $K = \frac{(\Delta\alpha/\Delta\delta)_3}{\Delta\alpha/\Delta\delta} = 1.0$. The 3 or 4 percent

increase in the aspect-ratio correction that might be expected from a qualitative study of lifting-surface theory (actual numerical values have not yet been calculated) may either be masked by the scatter of the data in figures 1 or 2 or may be counteracted by three-dimensional boundary-layer effects or by the effect of the vertical location of the trailing-vortex sheet (references 28 and 31).

Lifting-line theory indicates no change in aileron effectiveness with deflection of partial-span flaps. Some effect might be expected because of cross flow; however, figure 12 shows that the deflection of partial-span flaps generally has no consistent effect on aileron effectiveness.

The available data on the effect of sweep and taper (figs. 13 and 14) show that, insofar as aileron rolling moments are concerned, no large corrections are to be applied to lifting-line theory for the effects of taper and sweep. For wings of low taper (large values of λ), it appears that the aileron effectiveness is slightly greater if the wing is swept forward.

CONCLUDING REMARKS

The trends indicated by the analysis of available data on the effectiveness of ailerons without exposed overhang balance have been summarized in the form of a few approximate rules concerning the effectiveness parameter $\Delta\alpha/\Delta\delta$ (at constant lift): Thickening and beveling the trailing edge (as measured by the trailing-edge angle ϕ) will generally reduce the effectiveness about 0.3 percent per degree of bevel for ailerons sealed at the hinge axis and about 0.6 percent per degree of bevel for unsealed ailerons. A 0.005c gap at the hinge axis usually reduces the effectiveness about 17 percent for flap chord ratios of 0.2. This percentage increases as the flap chord ratio is reduced. The effectiveness is about 14 percent lower at aileron deflections of 20° than at aileron deflections of 10° . At large angles of attack ($\alpha = 10^\circ$) and for chord ratios of about 0.2, positively deflected ailerons are about 20 percent less

effective than negatively deflected ailerons. The deflection of partial-span flaps has no consistent effect on the effectiveness. Increases in Mach number and forward movement of the transition point decrease the aileron effectiveness.

No consistent correction to the lifting-line-theory method of estimating aileron rolling moments could be detected. Because the several factors neglected in lifting-line theory apparently are fairly small and counteract one another, on the average, no additional correction need be applied.

Langley Memorial Aeronautical Laboratory,
National Advisory Committee for Aeronautics,
Langley Field, Va.,

REFERENCES

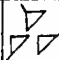
1. Street, William G., and Ames, Milton B., Jr.: Pressure-Distribution Investigation of an N.A.C.A. 0009 Airfoil with a 50-Percent-Chord Plain Flap and Three Tabs. NACA TN No. 734, 1939.
2. Ames, Milton B., Jr., and Sears, Richard I.: Pressure-Distribution Investigation of an N.A.C.A. 0009 Airfoil with an 80-Percent-Chord Plain Flap and Three Tabs. NACA TN No. 761, 1940.
3. Ames, Milton B., Jr., and Sears, Richard I.: Pressure-Distribution Investigation of an N.A.C.A. 0009 Airfoil with a 30-Percent-Chord Plain Flap and Three Tabs. NACA TN No. 759, 1940.
4. Sears, Richard I.: Wind-Tunnel Investigation of Control-Surface Characteristics. I - Effect of Gap on the Aerodynamic Characteristics of an NACA 0009 Airfoil with a 30-Percent-Chord Plain Flap. NACA ARR, June 1941.
5. Jones, Robert T., and Ames, Milton B., Jr.: Wind-Tunnel Investigation of Control-Surface Characteristics. V - The Use of a Beveled Trailing Edge to Reduce the Hinge Moment of a Control Surface. NACA ARR, March 1942.
6. Sears, Richard I., and Liddell, Robert B.: Wind-Tunnel Investigation of Control-Surface Characteristics. VI - A 30-Percent-Chord Plain Flap on the NACA 0015 Airfoil. NACA ARR, June 1942.
7. Gillis, Clarence L., and Lockwood, Vernard E.: Wind-Tunnel Investigation of Control-Surface Characteristics. XIII - Various Flap Overhangs Used with a 30-Percent-Chord Flap on an NACA 66-009 Airfoil. NACA ACR No. 3G20, 1943.
8. Sears, Richard I., and Hoggard, H. Page, Jr.: Wind-Tunnel Investigation of Control-Surface Characteristics. XI - Various Large Overhang and Internal-Type Aerodynamic Balances for a Straight-Contour Flap on the NACA 0015 Airfoil. NACA ARR, Jan. 1943.

9. Purser, Paul E., and Riebe, John M.: Wind-Tunnel Investigation of Control-Surface Characteristics. XV - Various Contour Modifications of a 0.30-Airfoil-Chord Plain Flap on an NACA 66(215)-014 Airfoil. NACA ACR No. 3L20, 1943.
10. Wenzinger, Carl J., and Delano, James B.: Pressure Distribution over an N.A.C.A. 23012 Airfoil with a Slotted and a Plain Flap. NACA Rep. No. 633, 1938.
11. Wenzinger, Carl J., and Harris, Thomas A.: Wind-Tunnel Investigation of an N.A.C.A. 23012 Airfoil with Various Arrangements of Slotted Flaps. NACA Rep. No. 664, 1939.
12. Crane, Robert M., and Holtzclaw, Ralph W.: Wind-Tunnel Investigation of Ailerons on a Low-Drag Airfoil. I - The Effect of Aileron Profile. NACA ACR No. 4A14, 1944.
13. Denaci, H. G., and Bird, J. D.: Wind-Tunnel Tests of Ailerons at Various Speeds. II - Ailerons of 0.20 Airfoil Chord and True Contour with 0.60 Aileron-Chord Sealed Internal Balance on the NACA 66,2-216 Airfoil. NACA ACR No. 3F18, 1943.
14. Davidson, Milton, and Turner, Harold R., Jr.: Tests of an NACA 66,2-216, $a = 0.6$ Airfoil Section with a Slotted and Plain Flap. NACA ACR No. 3J05, 1943.
15. Rogallo, F. M.: Collection of Balanced-Aileron Test Data. NACA ACR No. 4A11, 1944.
16. Rogallo, F. M., and Purser, Paul E.: Wind-Tunnel Investigation of 20-Percent-Chord Plain and Frise Ailerons on an NACA 23012 Airfoil. NACA ARR, Dec. 1941.
17. Rogallo, F. M., and Schuldenfrei, Marvin: Wind-Tunnel Investigation of a Plain and a Slot-Lip Aileron on a Wing with a Full-Span Flap Consisting of an Inboard Fowler and an Outboard Slotted Flap. NACA ARR, June 1941.

18. Weick, Fred E., and Wenzinger, Carl J.: Wind-Tunnel Research Comparing Lateral Control Devices, Particularly at High Angles of Attack. I - Ordinary Ailerons on Rectangular Wings. NACA Rep. No. 419, 1932.
19. Weick, Fred E., and Shortal, Joseph A.: Wind-Tunnel Research Comparing Lateral Control Devices, Particularly at High Angles of Attack. V - Spoilers and Ailerons on Rectangular Wings. NACA Rep. No. 439, 1932.
20. Weick, Fred E., and Shortal, Joseph A.: Wind-Tunnel Research Comparing Lateral Control Devices, Particularly at High Angles of Attack. VIII. Straight and Skewed Ailerons on Wings with Rounded Tips. NACA TN No. 445, 1933.
21. Weick, Fred E., and Wenzinger, Carl J.: Wind-Tunnel Research Comparing Lateral Control Devices, Particularly at High Angles of Attack. IX. Tapered Wings with Ordinary Ailerons. NACA TN No. 449, 1933.
22. Wenzinger, Carl J.: Wind-Tunnel Investigation of Tapered Wings with Ordinary Ailerons and Partial-Span Split Flaps. NACA Rep. No. 611, 1937.
23. Wenzinger, Carl J., and Ames, Milton B., Jr.: Wind-Tunnel Investigation of Rectangular and Tapered N.A.C.A. 23012 Wings with Plain Ailerons and Full-Span Split Flaps. NACA TN No. 661, 1938.
24. Irving, H. B., and Batson, A. S.: A Comparison of Aileron Control on Tapered Wings with Straight Leading Edge and Straight Trailing Edge. R. & M. No. 1837, British A.R.C., 1938.
25. Weick, Fred E., and Jones, Robert T.: Résumé and Analysis of N.A.C.A. Lateral Control Research. NACA Rep. No. 605, 1937.
26. Pearson, Henry A., and Jones, Robert T.: Theoretical Stability and Control Characteristics of Wings with Various Amounts of Taper and Twist. NACA Rep. No. 635, 1938.

27. Anderson, Raymond F.: Determination of the Characteristics of Tapered Wings. NACA Rep. No. 572, 1936.
28. Swanson, Robert S., and Gillis, Clarence L.: Limitations of Lifting-Line Theory for Estimation of Aileron Hinge-Moment Characteristics. NACA CB No. 3LC2, 1943.
29. Cohen, Boris: A Method for Determining the Camber and Twist of a Surface to Support a Given Distribution of Lift. NACA TN No. 855, 1942.
30. Jones, Robert T.: Theoretical Correction for the Lift of Elliptic Wings. Jour. Aero. Sci., vol. 9, no. 1, Nov. 1941, pp. 8-10.
31. Bollay, William: A Non-linear Wing Theory and its Application to Rectangular Wings of Small Aspect Ratio. Z.f.a.M.M., Ed. 19, Heft 1, Feb. 1939, pp. 21-35.
32. Jacobs, Eastman N., Abbott, Ira H., and Davidson, Milton: Supplement (loose-leaf) to NACA Advance Confidential Report, Preliminary Low-Drag-Airfoil and Flap Data from Tests at Large Reynolds Numbers and Low Turbulence. NACA, March 1942.

TABLE I.- SUPPLEMENTARY INFORMATION REGARDING
TESTS OF TWO-DIMENSIONAL MODELS

Model		Basic airfoil	Type of flap	Air-flow characteristics			Published reference
Design- nation	Sym- bol			τ	M	R	
1	○	NACA 0009	Plain	1.93	0.08	-----	1 to 5
2a	+	NACA 0015	Plain	1.93	0.10	1.4×10^6	6
2b		NACA 0015	Internally balanced, straight contour	1.93	0.10	1.4×10^6	8
3	×	NACA 23012	Plain	1.60	0.11	2.2×10^6	10,11
4	□	NACA 66(2x15)-009	Plain, straight contour	1.93	0.10	1.4×10^6	-----
5	◇	NACA 66-009	Plain	1.93	0.11	1.4×10^6	7
6	△	NACA low drag	Internally balanced	Approach- ing 1.00	0.17	2.5×10^6	15
7	▽	NACA 66(2x15)-216, a = 0.6	Internally balanced	Approach- ing 1.00	0.18	5.3×10^6	15
8	▷	NACA 66(2x15)-116, a = 0.6	Internally balanced	Approach- ing 1.00	0.14	6.0×10^6	15
9	◁	NACA compromise low drag	Plain	Approach- ing 1.00	-----	13.0×10^6	-----
10	◁	NACA low drag	Internally balanced	Approach- ing 1.00	0.14	6.0×10^6	15
11	▽	NACA 63(1420)-521 (approx.)	Internally balanced	Approach- ing 1.00	-----	8.0×10^6	-----
12	◁	^a NACA 66(215)-216, a = 0.6	Internally balanced	Approach- ing 1.00	0.20 to 0.48	2.8×10^6 to 6.8×10^6	13
13	○	^a NACA 66(215)-216, a = 0.6	Plain	Approach- ing 1.00	0.14	3.8×10^6	12
14	◁	NACA 66(215)-0114	Plain	1.93	0.09	1.2×10^6	9
15	○	NACA 66,2-216, a = 0.6	Plain	Approach- ing 1.00	-----	6.0×10^6	14

^aThis designation has been changed from the form in which it appears in reference to the form described on p. 21a of reference 32.

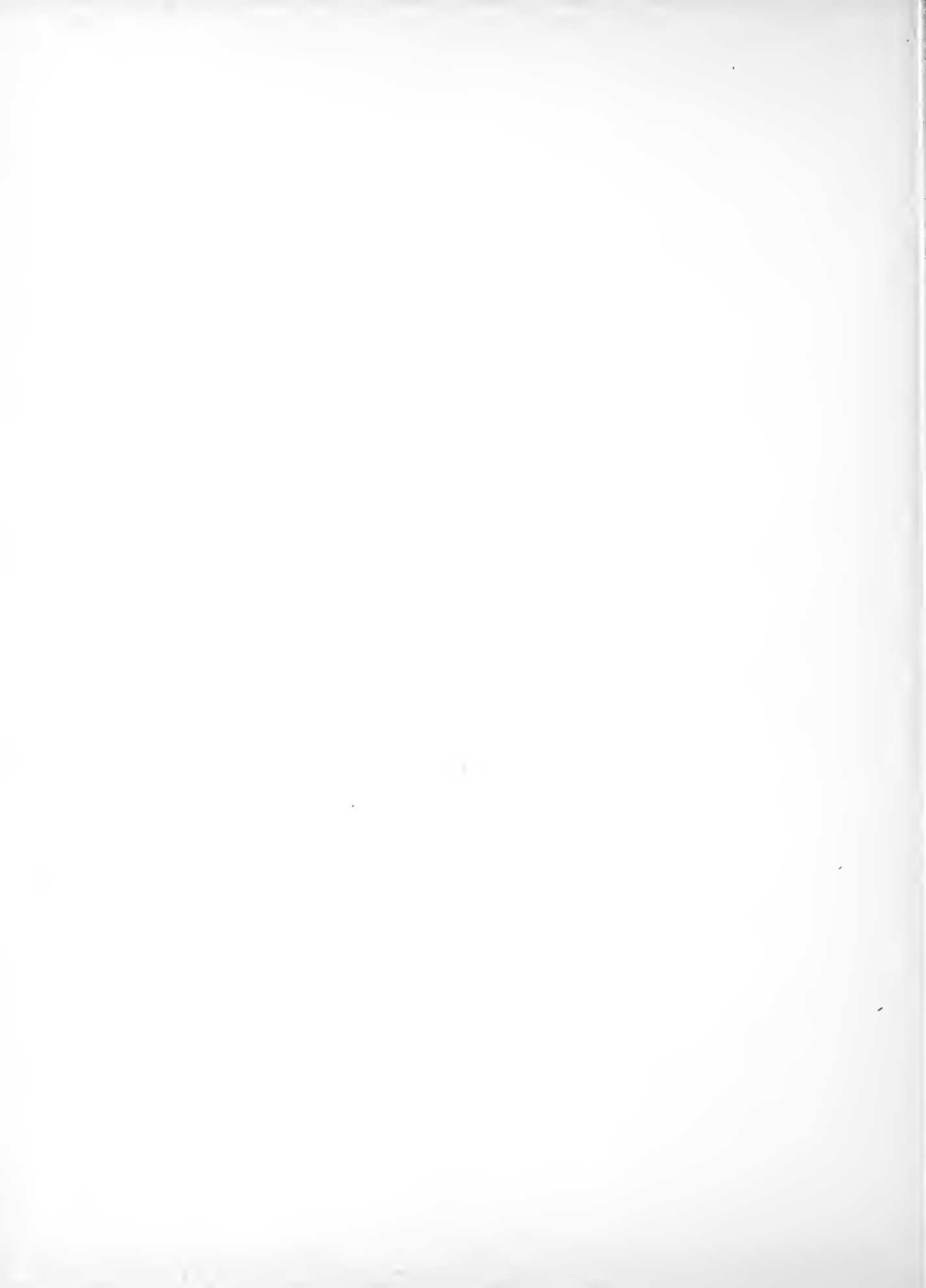


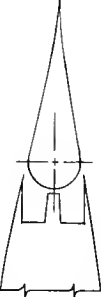




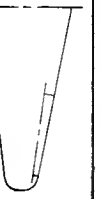



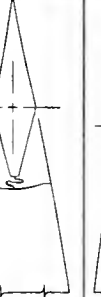








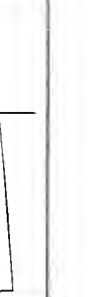


TABLE II.- SUPPLEMENTARY INFORMATION REGARDING TESTS OF THREE-DIMENSIONAL MODELS

Designation	Model		Typical airfoil section	Airfoil section		Λ	λ	Aileron location		α_e/α	Estimated slope of section lift curve, per deg		Air-flow characteristics	Reference published
	Symbol	Plan form		Root	Tip			$\frac{y_1}{b/2}$	$\frac{y_2}{b/2}$		Gap sealed	Gap unsealed		
16				NACA 65(228)-118, $a = 1.0$	NACA 65(216)-115, $a = 0.5$	12.0	0.32	0.641	0.945	0.228	0.110	0.107	$R = 1.99 \times 10^6$ $M = 0.11$ $\gamma = 1.6$	---
17a				NACA 66,2-118, $a = 1.0$	NACA 66(2x15)-116, $a = 1.0$	6.23	0.33	0.490	0.906	0.119	0.103	-----	$R = 1.9 \times 10^6$ $M = 0.11$ $\gamma = 1.6$	15
17b				NACA 66,2-118, $a = 1.0$	NACA 66(2x15)-116, $a = 1.0$	6.23	0.33	0.490	0.906	0.162	0.103	-----	$R = 1.9 \times 10^6$ $M = 0.11$ $\gamma = 1.6$	15
17c				NACA 66,2-118, $a = 1.0$	NACA 66(2x15)-116, $a = 1.0$	6.23	0.33	0.490	0.977	0.149	0.103	-----	$R = 1.9 \times 10^6$ $M = 0.11$ $\gamma = 1.6$	15
17d				NACA 66,2-118, $a = 1.0$	NACA 66(2x15)-116, $a = 1.0$	6.23	0.33	0.490	0.906	0.175	0.103	-----	$R = 1.9 \times 10^6$ $M = 0.11$ $\gamma = 1.6$	15
17e				NACA 66,2-118, $a = 1.0$	NACA 66(2x15)-116, $a = 1.0$	6.23	0.33	0.490	0.977	0.039	0.103	-----	$R = 1.9 \times 10^6$ $M = 0.11$ $\gamma = 1.6$	15
18a				NACA 23015.5 (approx.)	NACA 23008.25 (approx.)	5.55	0.60	0.579	0.984	0.155	0.105	0.103	$R = 1.54 \times 10^6$ $M = 0.08$ $\gamma = 1.6$	15

CONFIDENTIAL

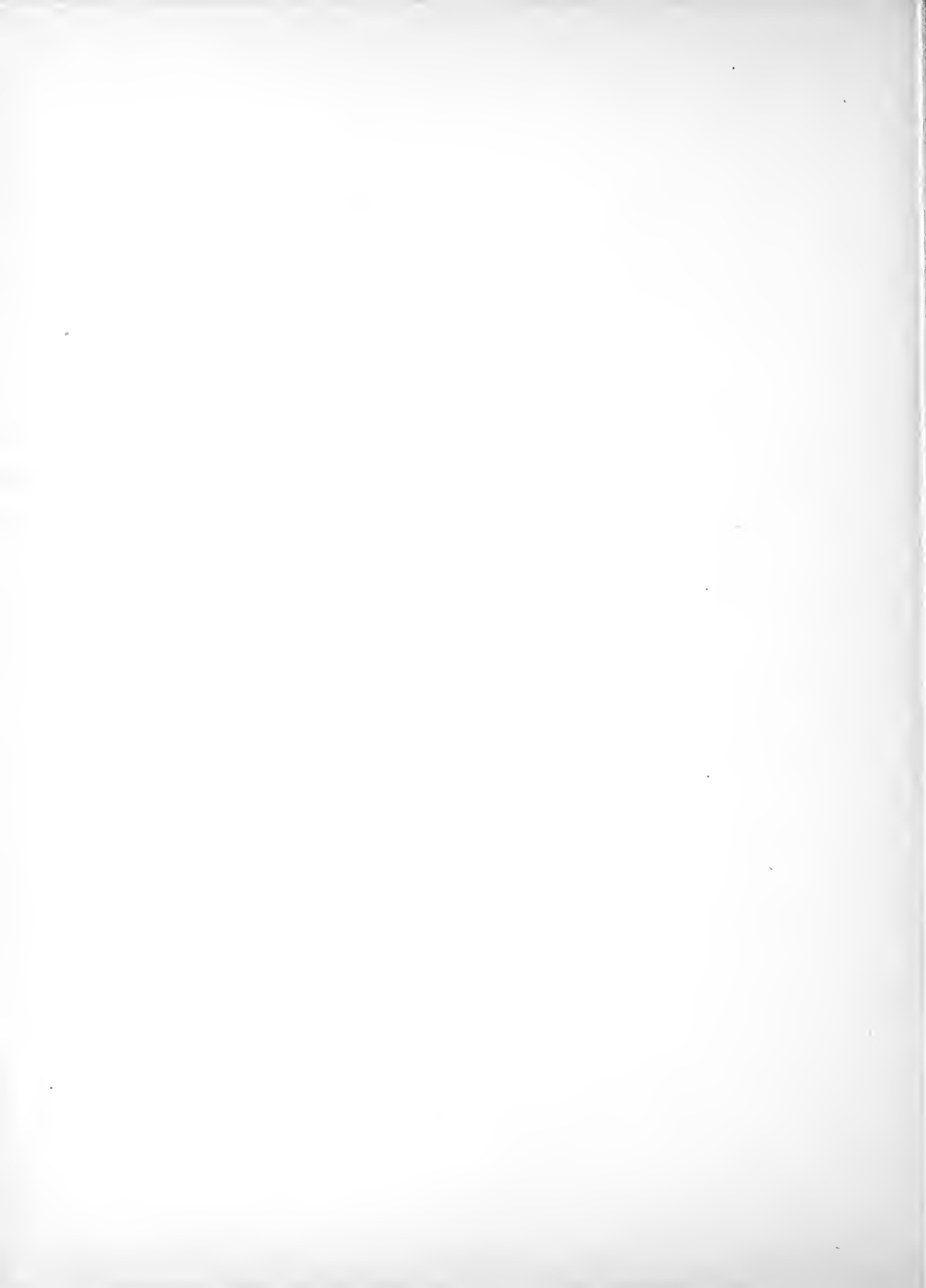


TABLE II.- SUPPLEMENTARY INFORMATION - Continued

Design- notation	Model		Typical airfoil section	Airfoil section		A	λ	Alleron location		c_e/o	Estimated slope of section lift curve, per deg		Air-flow characteristics	Published Reference
	Symbol	Plan form		Root	Tip			$\frac{y_L}{b/2}$	$\frac{y_c}{b/2}$		Gap sealed	Gap unsealed		
18b				NACA 23015.5 (approx.)	NACA 23008.25 (approx.)	5.55	0.60	0.579	0.984	0.155	0.105	-----	$R = 1.54 \times 10^6$ $M = 0.08$ $\gamma = 1.6$	15
18a				NACA 23015.5 (approx.)	NACA 23008.25 (approx.)	5.55	0.60	0.579	0.984	0.031	0.105	0.103	$R = 1.54 \times 10^6$ $M = 0.08$ $\gamma = 1.6$	15
18d				NACA 23015.5 (approx.)	NACA 23008.25 (approx.)	5.55	0.60	0	0.984	0.080	0.105	0.103	$R = 2.05 \times 10^6$ $M = 0.11$ $\gamma = 1.6$	15
19a				NACA 23012		4.00	1.00	0.630	1.000	0.200	0.105	-----	$R = 1.5 \times 10^6$ $M = 0.06$ $\gamma = 1.6$	16
19b				NACA 23012		4.00	1.00	0.630	1.000	0.150	0.105	-----	$R = 1.5 \times 10^6$ $M = 0.06$ $\gamma = 1.6$	15
19c				NACA 23012		4.00	1.00	0.630	1.000	0.100	0.105	0.103	$R = 1.5 \times 10^6$ $M = 0.06$ $\gamma = 1.6$	17
20a				NACA low drag		7.30	0.42	0.509	0.980	0.192	0.103	0.101	$R = 2.35 \times 10^6$ $M = 0.11$ $\gamma = 1.6$	15

CONFIDENTIAL

CONFIDENTIAL

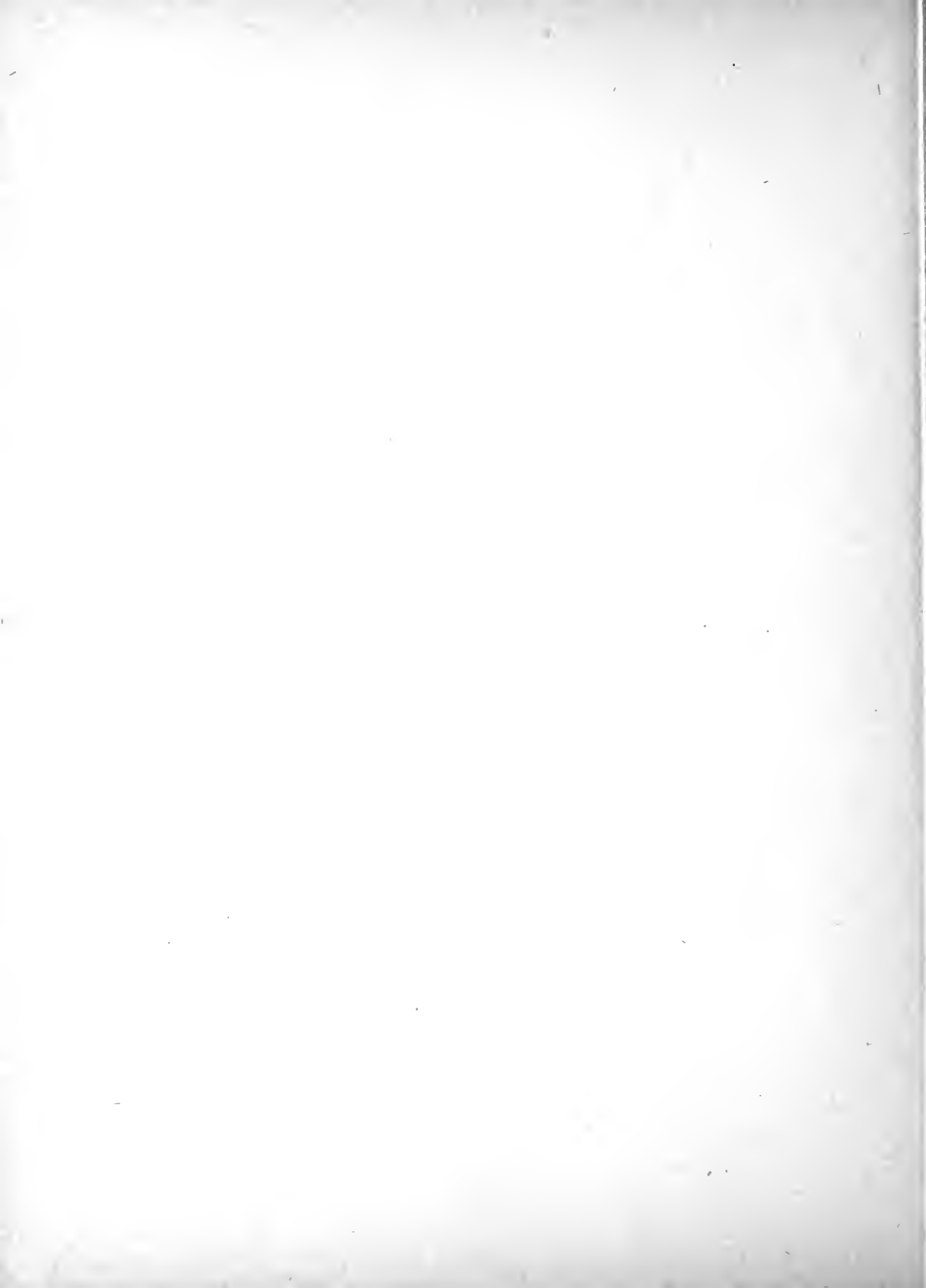

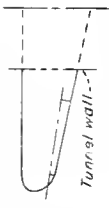
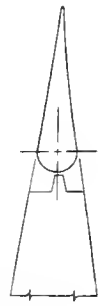

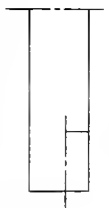
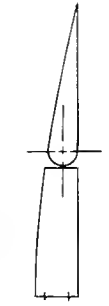


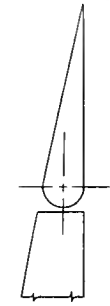

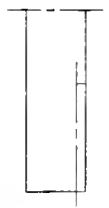
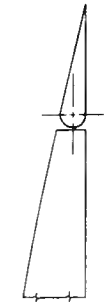

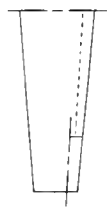
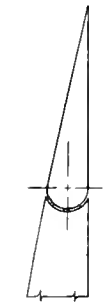

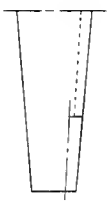


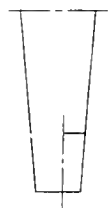
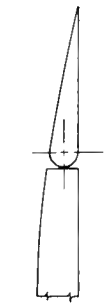


TABLE II.- SUPPLEMENTARY INFORMATION - Continued


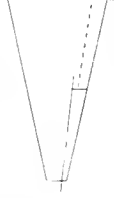


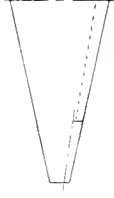


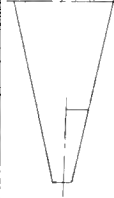
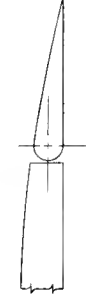

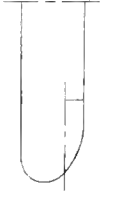
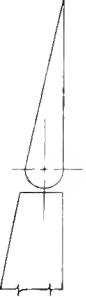

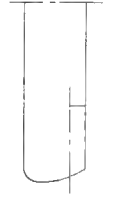
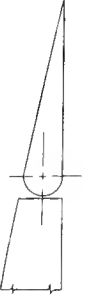


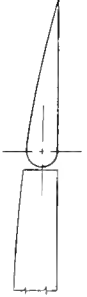


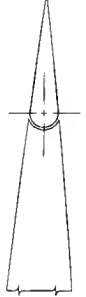
Designation	Model		Typical airfoil section	Airfoil section		A	λ	Alleron location			Estimated slope of section lift curve, per deg	Air-flow characteristics	Published reference
	Symbol	Plan form		Root	Tip			$y_1/b/2$	$y_2/b/2$	α_0/α			
20b				NACA low drag		7.30	0.42	0.509	0.933	0.200	0.103	$R = 2.35 \times 10^6$ $M = 0.11$ $\gamma = 1.6$	---
21a				Clark Y		6.00	1.00	0.70	1.000	0.40	0.097	$R = 0.61 \times 10^6$ $M = 0.11$ $\gamma = 1.4$	18 19
21b				Clark Y		6.00	1.00	0.60	1.000	0.25	0.097	$R = 0.61 \times 10^6$ $M = 0.11$ $\gamma = 1.4$	18 19
21c				Clark Y		6.00	1.00	0.40	1.000	0.15	0.097	$R = 0.61 \times 10^6$ $M = 0.11$ $\gamma = 1.4$	18
22a				Clark Y		6.00	0.60	0.700	1.000	0.250	0.102	$R = 0.61 \times 10^6$ $M = 0.11$ $\gamma = 1.4$	22
22b				Clark Y		6.00	0.60	0.550	1.000	0.250	0.102	$R = 0.61 \times 10^6$ $M = 0.11$ $\gamma = 1.4$	21 22
22c				Clark Y		6.00	0.60	0.684	1.000	0.100	0.097	$R = 0.61 \times 10^6$ $M = 0.11$ $\gamma = 1.4$	21

CONFIDENTIAL

CONFIDENTIAL



TABLE II.- SUPPLEMENTARY INFORMATION - Continued

Design- notation	Model		Typical airfoil section	Airfoil section		A	λ	Airfoil location		c_m/c	Estimated slope of section lift curve, per deg		Air-flow characteristics	Published reference
	Symbol	Plan form		Root	Tip			$y_1/b/2$	$y_2/b/2$		Gap sealed	Gap unsealed		
23a				Clark Y		6.00	0.20	0.500	1.000	0.250	0.102	0.097	$R = 0.61 \times 10^6$ $M = 0.11$ $\gamma = 1.4$	21 22
23b				Clark Y		6.00	0.20	0.700	1.000	0.250	0.102	-----	$R = 0.61 \times 10^6$ $M = 0.11$ $\gamma = 1.4$	22
23c				Clark Y		6.00	0.20	0.600	1.000	0.400	-----	0.097	$R = 0.61 \times 10^6$ $M = 0.11$ $\gamma = 1.4$	23
24				Clark Y		6.00	1.00	0.510	0.910	0.235	-----	0.097	$R = 0.61 \times 10^6$ $M = 0.11$ $\gamma = 1.4$	20
25a				Clark Y		6.00	1.00	0.573	0.973	0.243	-----	0.097	$R = 0.61 \times 10^6$ $M = 0.11$ $\gamma = 1.4$	20
25b				Clark Y		6.00	1.00	0.685	0.985	0.117	-----	0.097	$R = 0.61 \times 10^6$ $M = 0.11$ $\gamma = 1.4$	20
26a				NACA 23012		6.00	1.000	0.400	1.000	0.150	0.102	-----	$R = 0.61 \times 10^6$ $M = 0.11$ $\gamma = 1.6$	23

CONFIDENTIAL

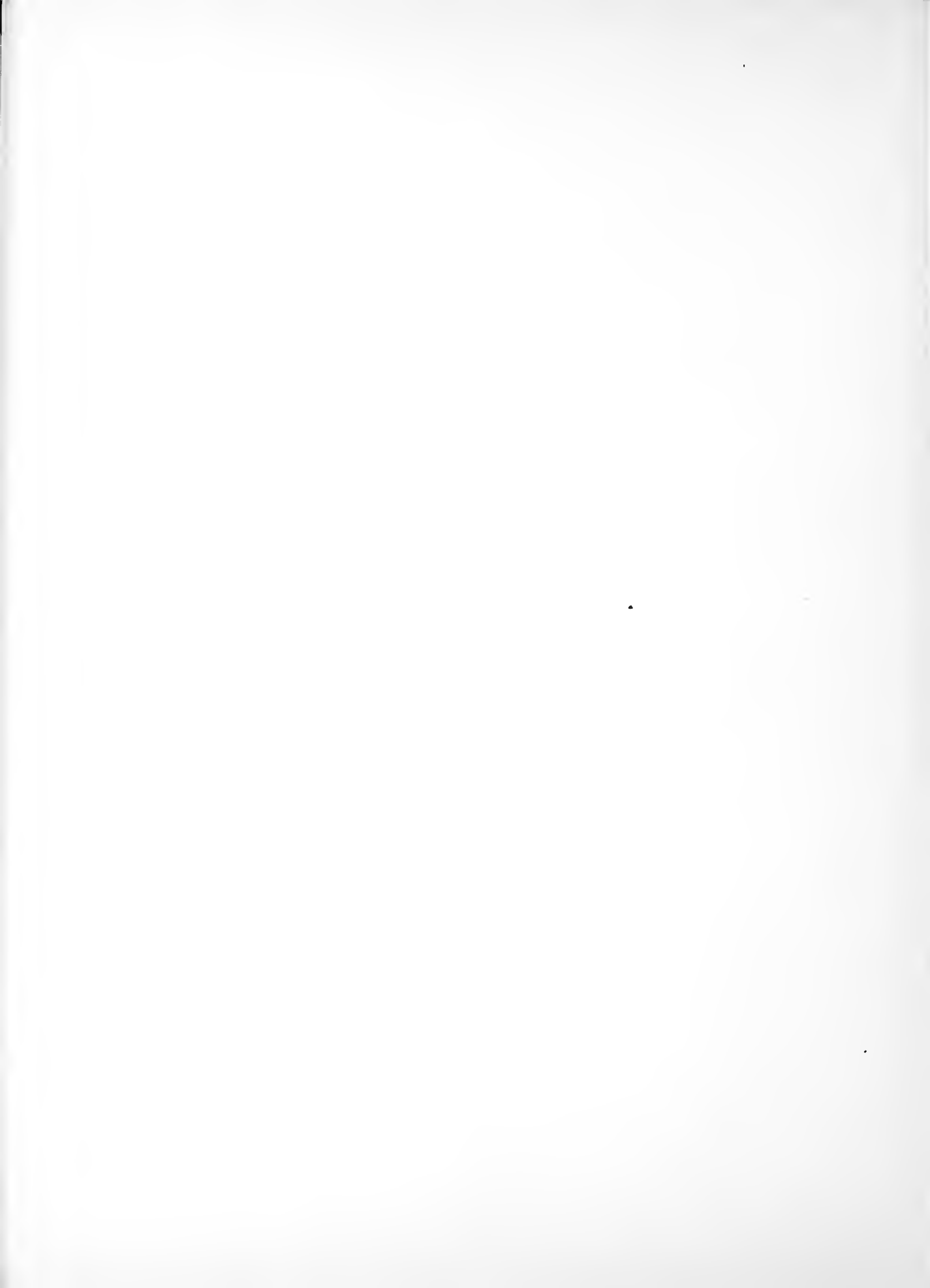


TABLE II.- SUPPLEMENTARY INFORMATION - Concluded

Designation	Model		Typical aileron section	Aileron section		A	λ	Aileron location			$c_{a/c}$	Estimated slope of section lift curve, per deg		Air-flow characteristics	Reference
	Symbol	Plan form		Root	Tip			$y_1/b/2$	$y_2/b/2$			Gap sealed	Gap unsealed		
26b				NACA 23012		6.00	1.000	0	1.000	0.100	0.102	-----	-----	$R = 0.61 \times 10^6$ $M = 0.11$ $\gamma = 1.6$	23
27				NACA 23012		6.00	0.200	0.400	1.000	0.150	0.102	-----	-----	$R = 0.61 \times 10^6$ $M = 0.11$ $\gamma = 1.6$	23
28				R.A.F. 38		7.2	0.400	0.600	1.000	0.250	-----	-----	-----	$R = 0.17 \times 10^6$ $M = 0.05$	24
29				R.A.F. 38		7.2	0.400	0.600	1.000	0.250	-----	-----	-----	$R = 0.17 \times 10^6$ $M = 0.05$	24
30				R.A.F. 38		7.2	0.250	0.600	1.000	0.250	-----	-----	-----	$R = 0.17 \times 10^6$ $M = 0.05$	24
31				R.A.F. 38		7.2	0.250	0.600	1.000	0.250	-----	-----	-----	$R = 0.17 \times 10^6$ $M = 0.05$	24

CONFIDENTIAL



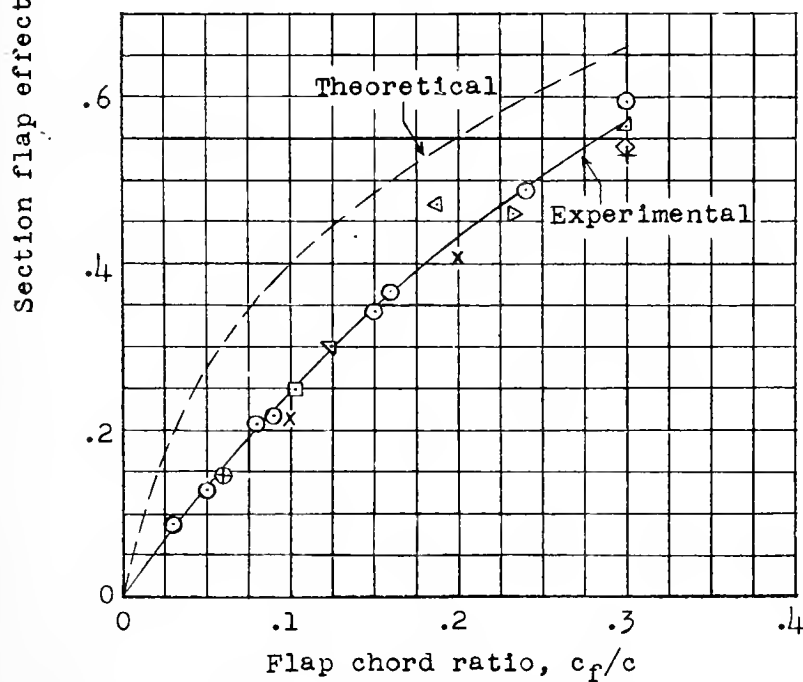
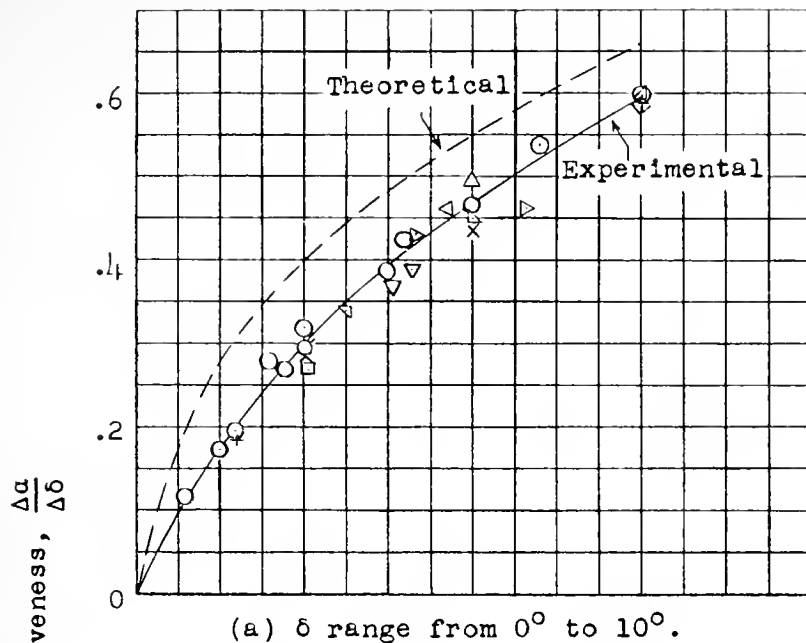


Figure 1.- Variation of section flap effectiveness with flap chord ratio for small Mach numbers and a small range of trailing-edge angle. Gaps sealed; $c_l = 0$. (Symbols designating two-dimensional models are identified in table I.)



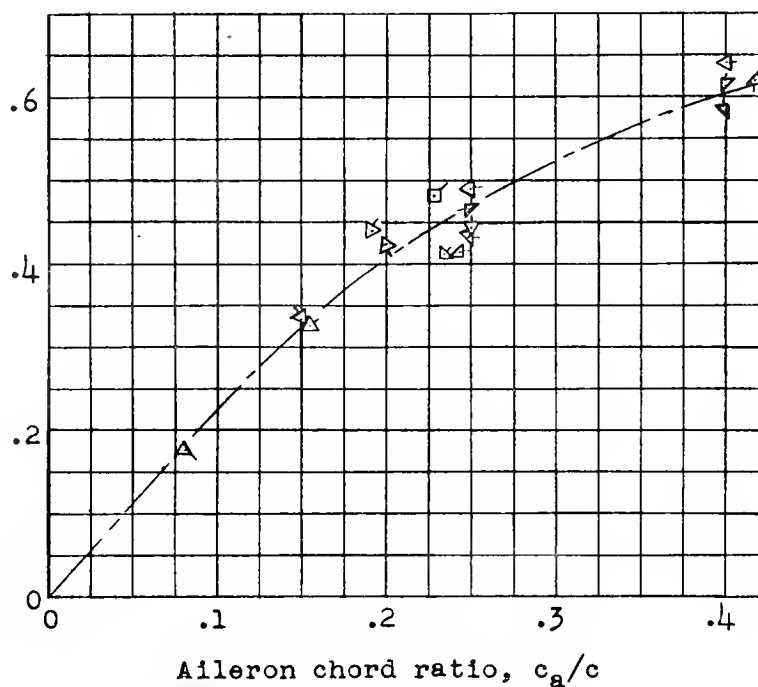
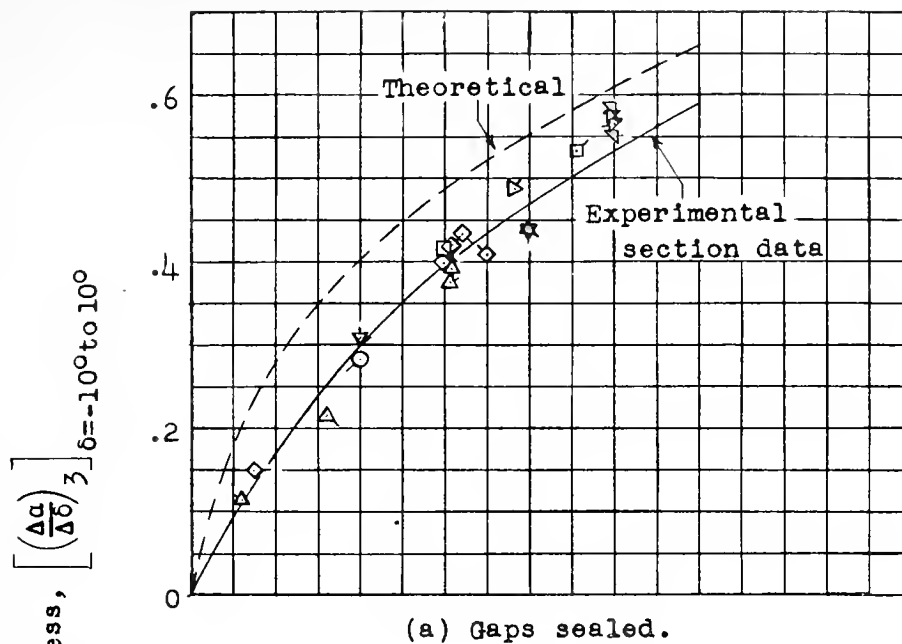


Figure 2.- Variation of aileron effectiveness with aileron chord ratio for small Mach numbers and a small range of trailing-edge angle. $\alpha \approx 0^\circ$. (Symbols designating three-dimensional models are identified in table II.)

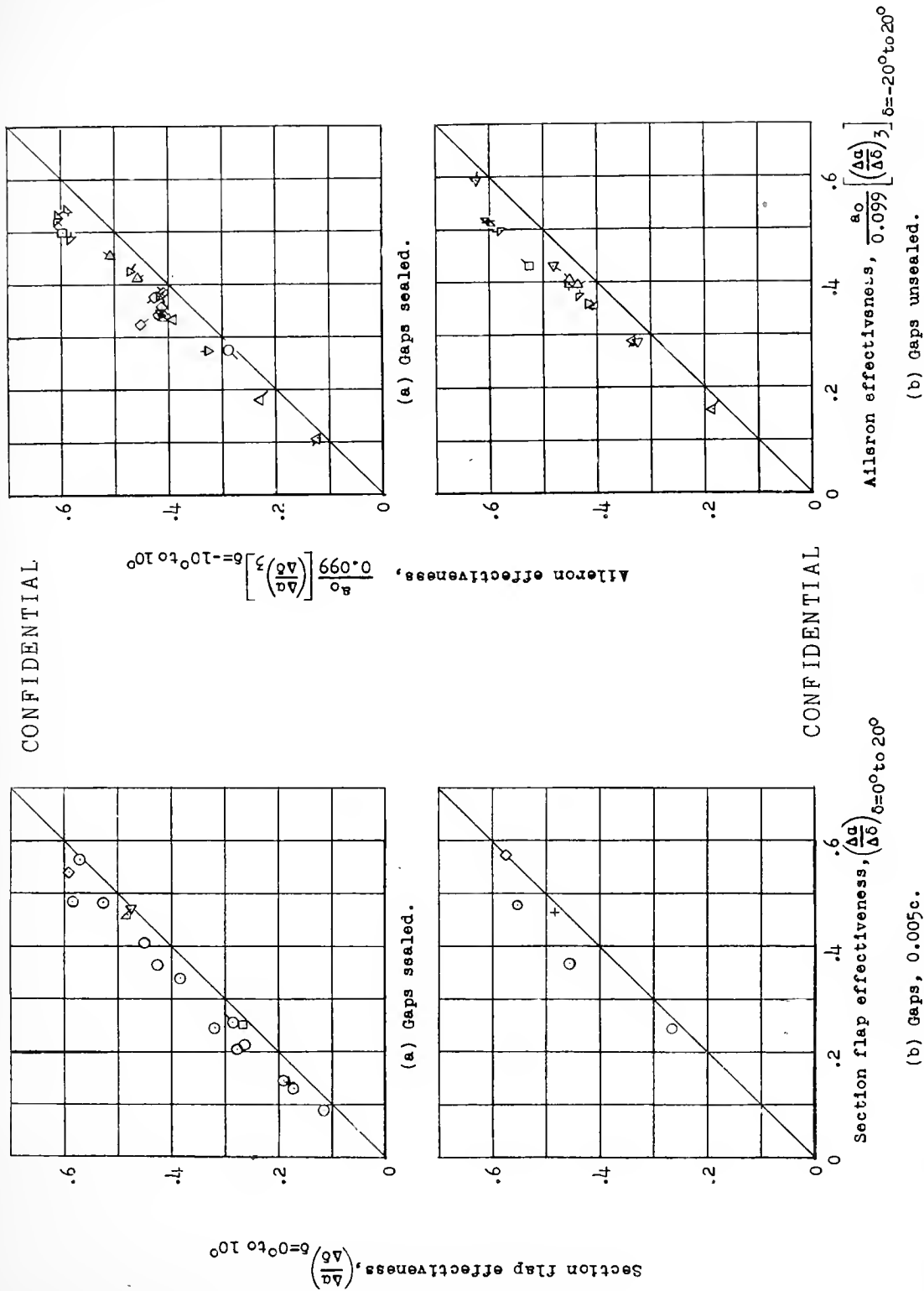
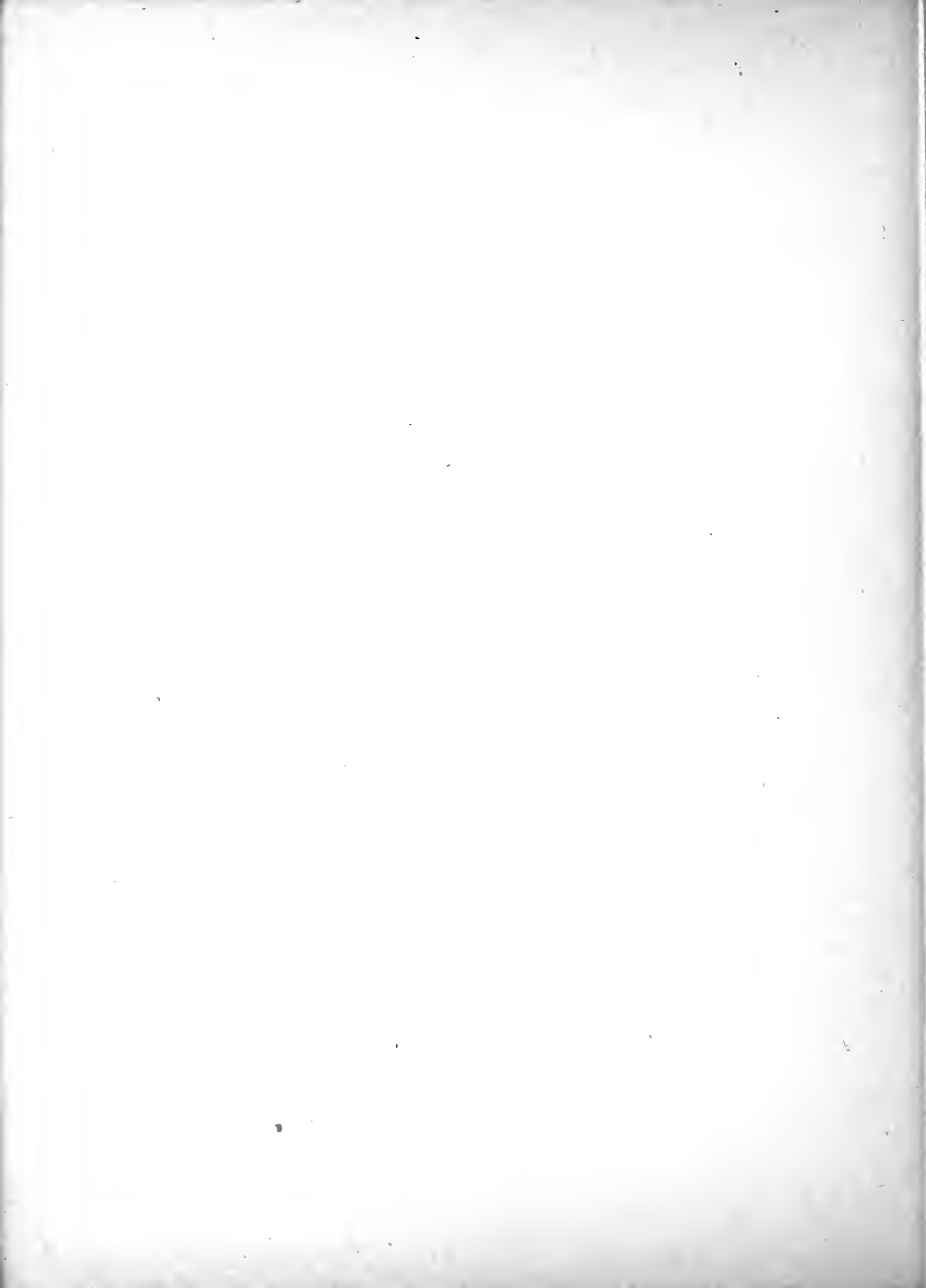


Figure 4.- Comparison of aileron effectiveness at large and small aileron deflections. $\alpha \approx 0^\circ$.

Figure 3.- Comparison of section flap effectiveness at large and small flap deflections. $c_l \approx 0$.



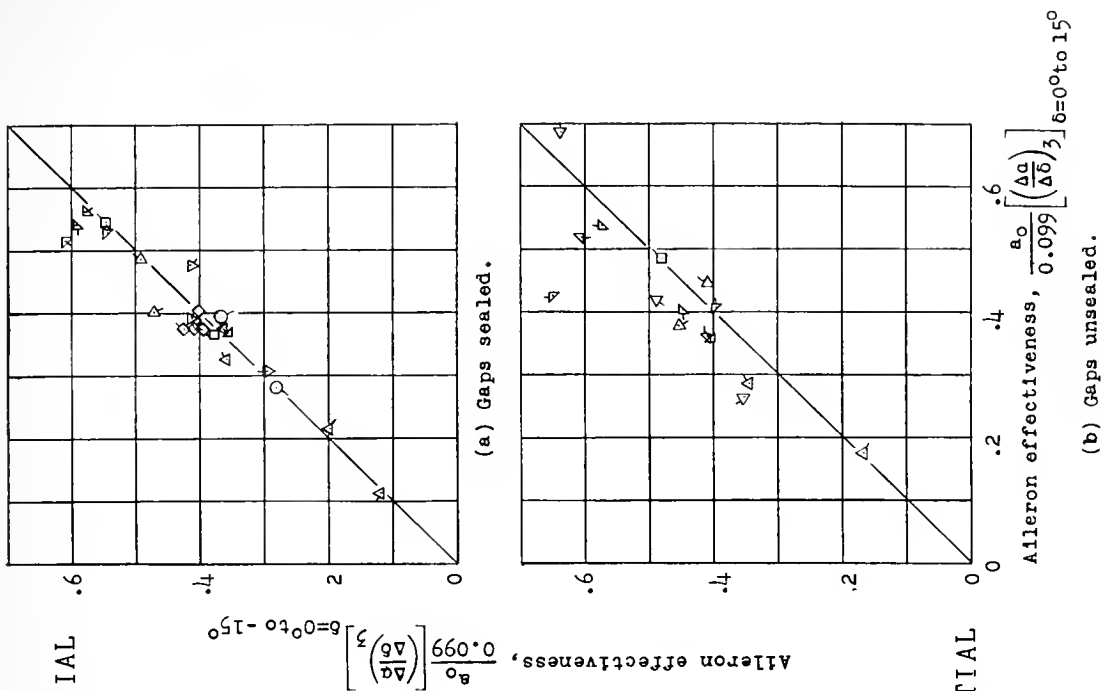


Figure 6.- Comparison of aileron effectiveness at positive and negative aileron deflections. $\alpha \approx 0^\circ$.

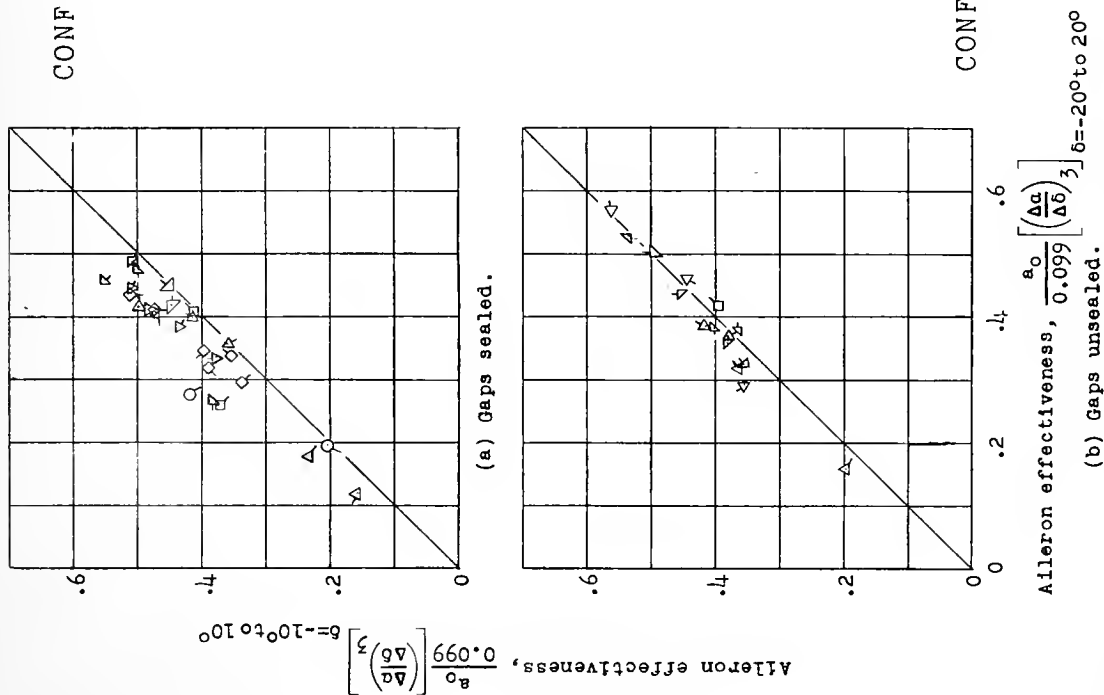
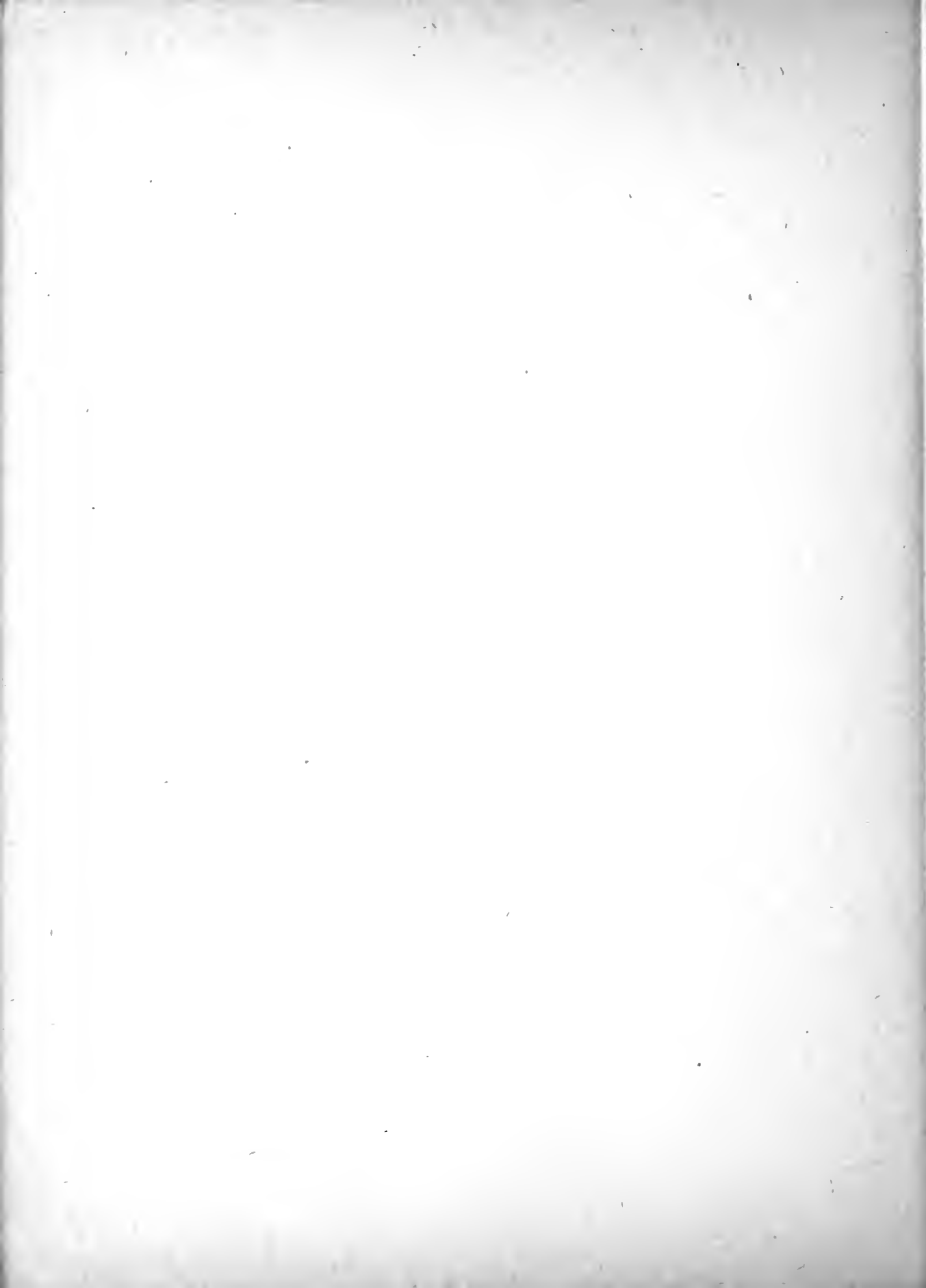


Figure 5.- Comparison of aileron effectiveness at large and small aileron deflections. $\alpha \approx 10^\circ$.



CONFIDENTIAL

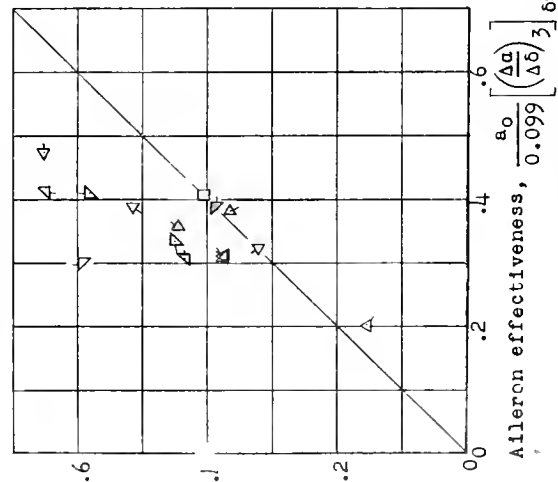
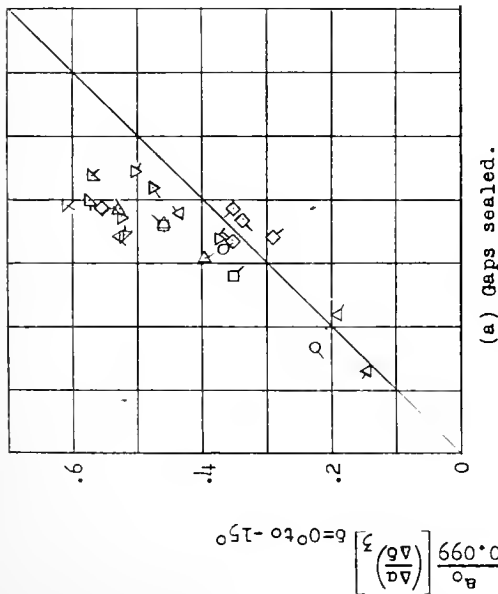


Figure 7.- Comparison of aileron effectiveness at positive and negative aileron deflections. $a \approx 10^\circ$.

Section flap effectiveness, $\frac{\Delta a}{\Delta \delta}$ with sealed gaps

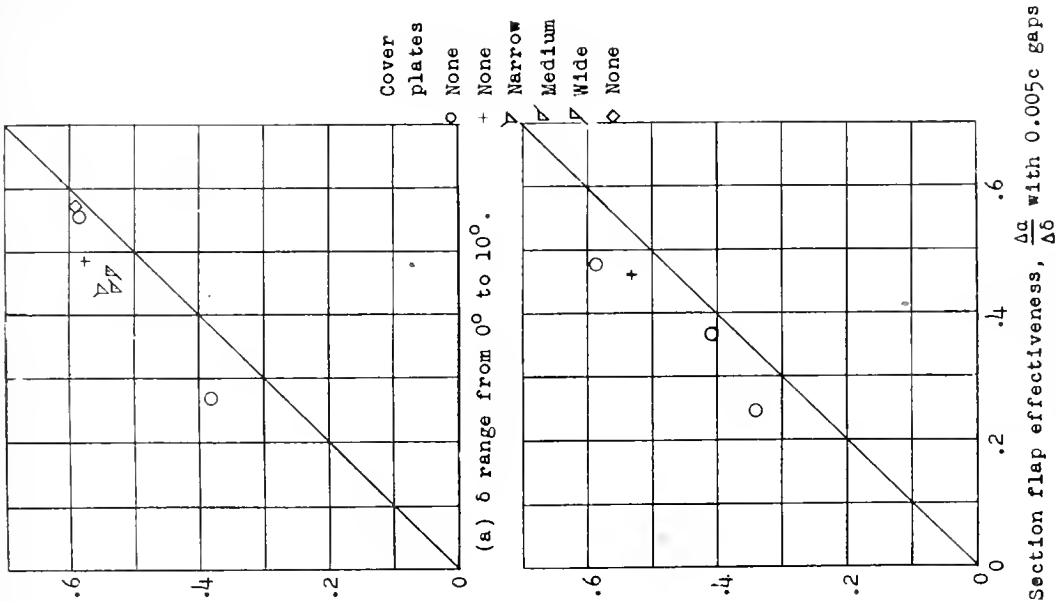
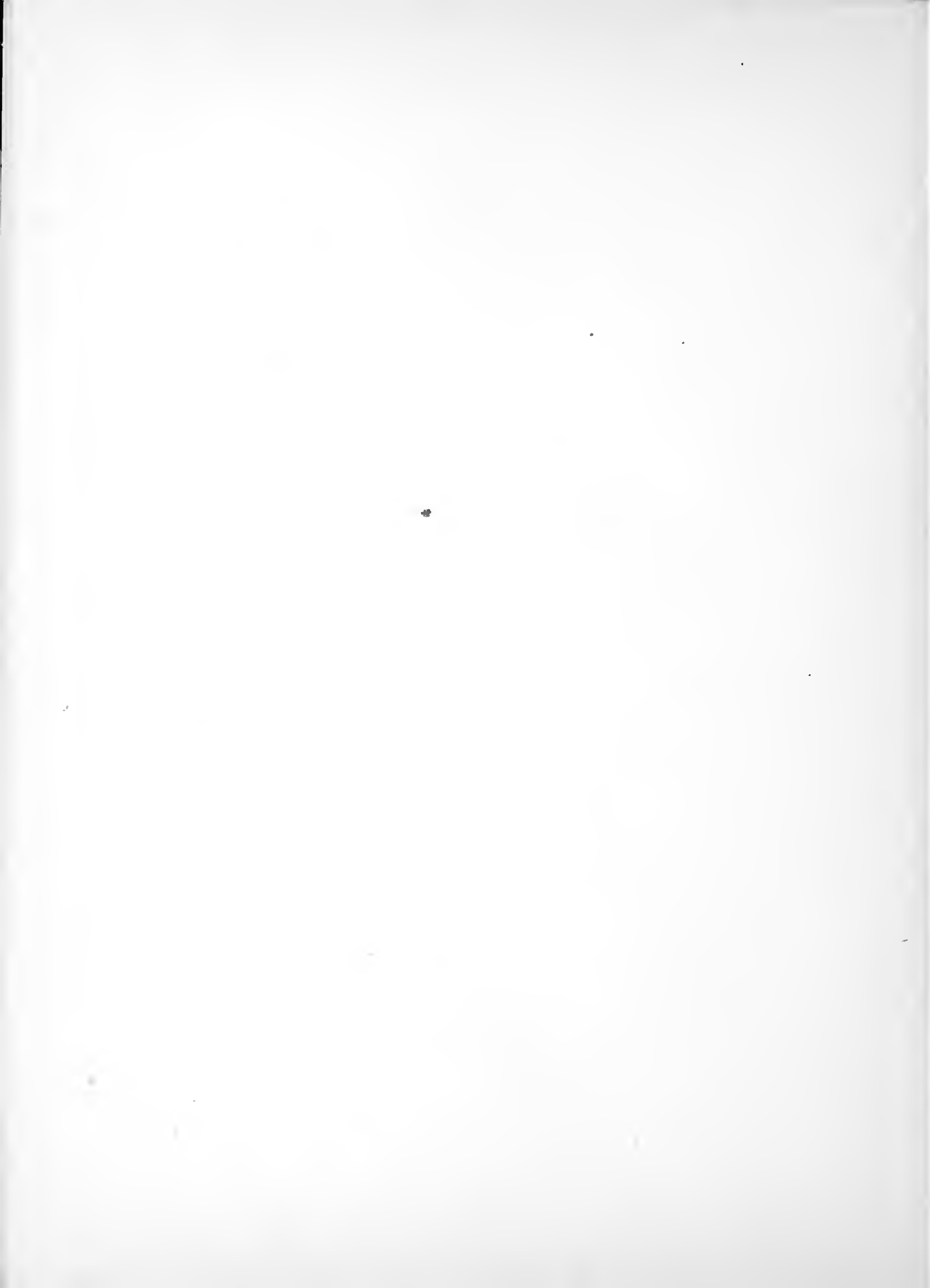


Figure 8.- Comparison of section flap effectiveness with gaps at hinge axis sealed and unsealed. $c_l = 0$.



CONFIDENTIAL

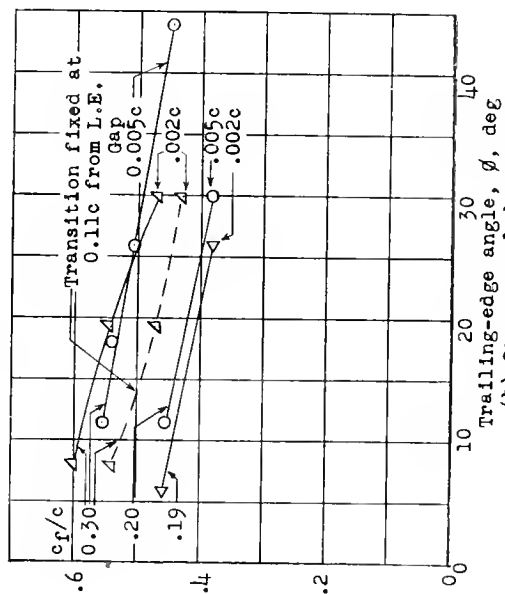
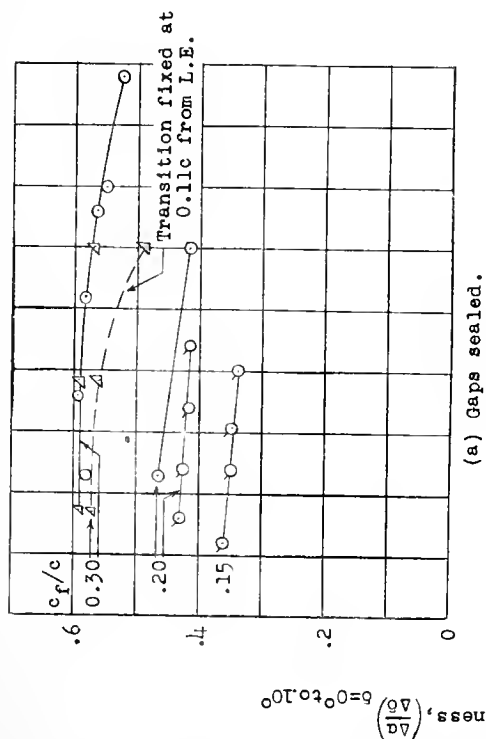


Figure 9.- Variation of section flap effectiveness with trailing-edge angle. $C_l = 0$.

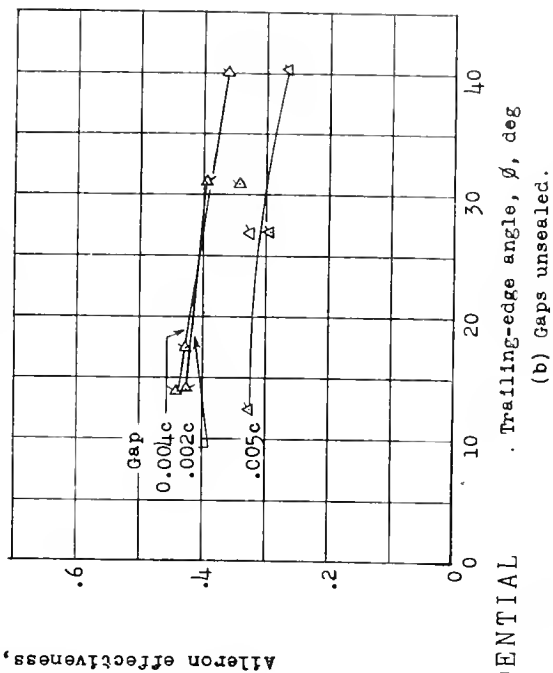
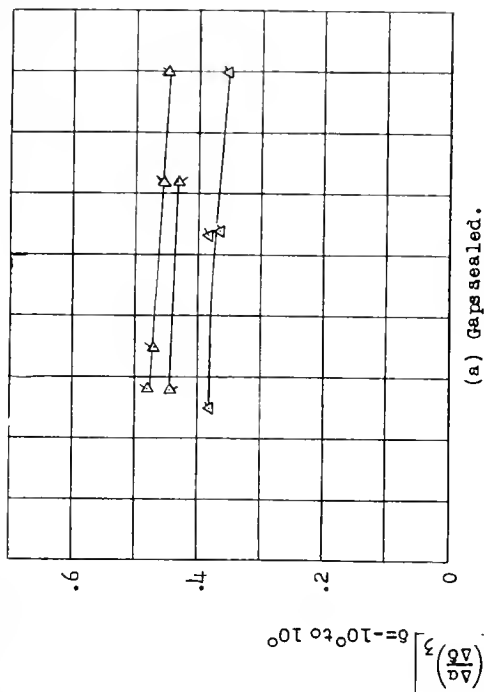
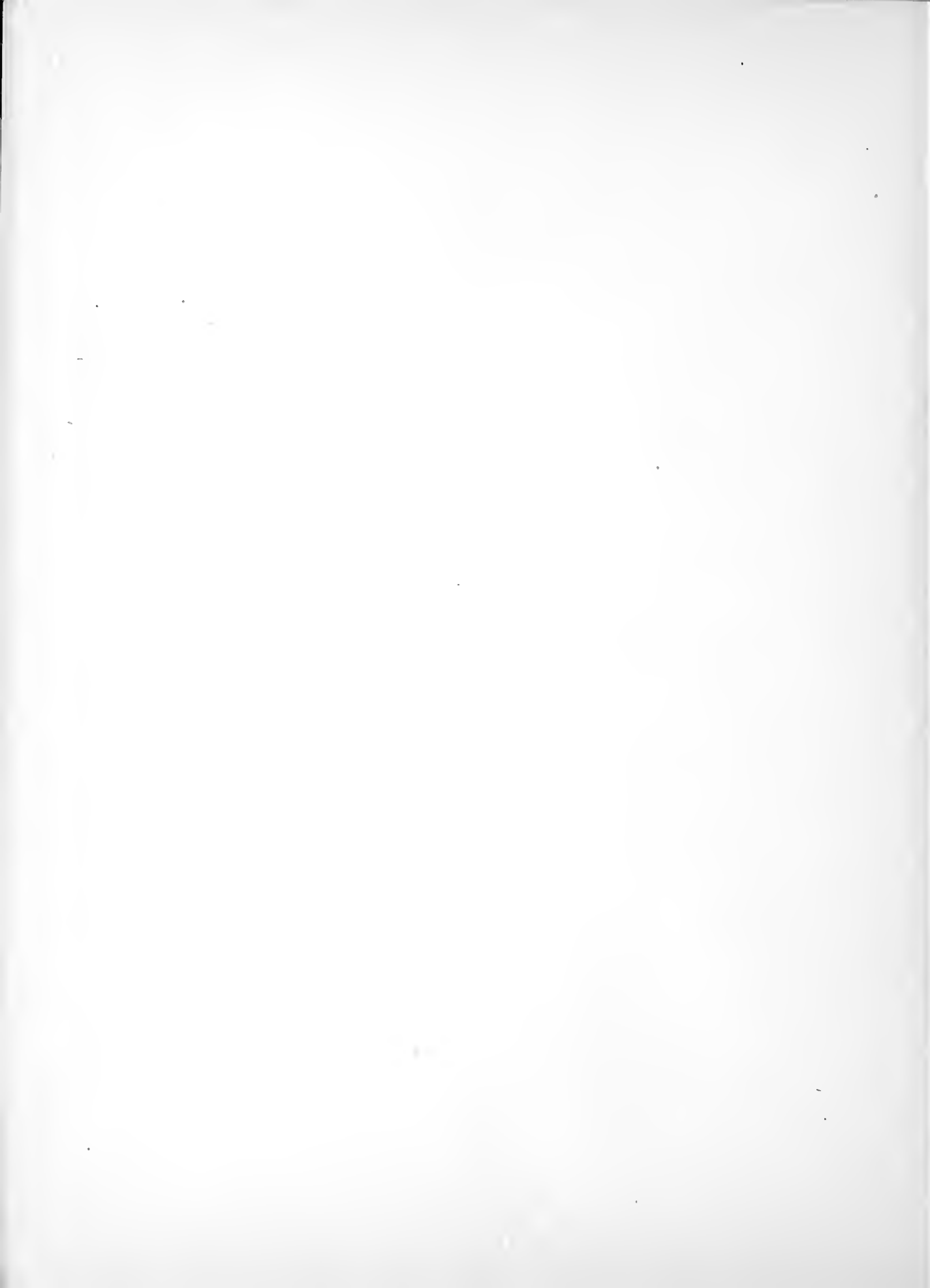


Figure 10.- Variation of aileron effectiveness with trailing-edge angle. $\alpha \approx 0^\circ$.

CONFIDENTIAL



CONFIDENTIAL

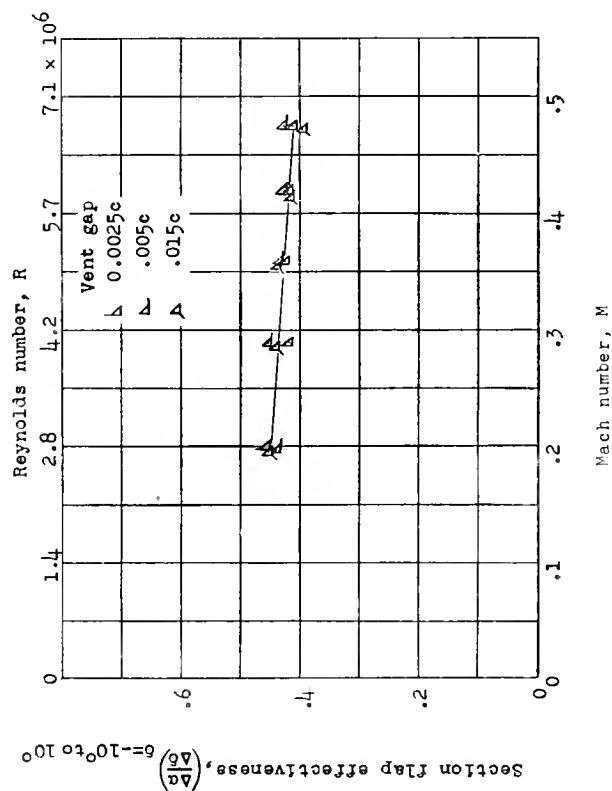


Figure 11.- Variation of section flap effectiveness with Mach number and Reynolds number. Model 12; sealed internal balance; $c_l = 0$.

CONFIDENTIAL

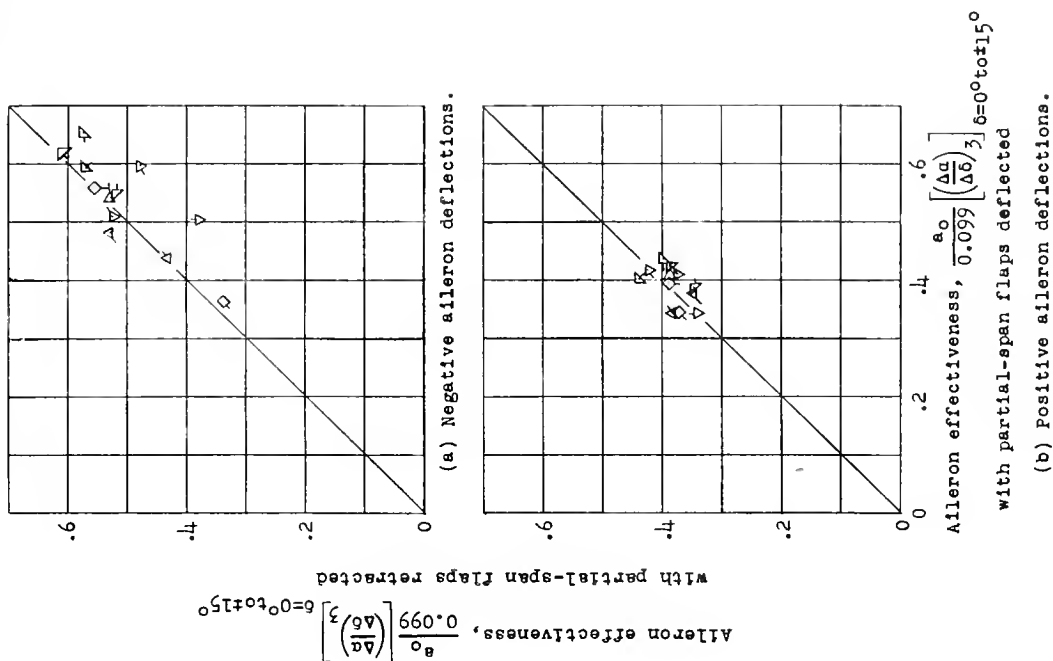
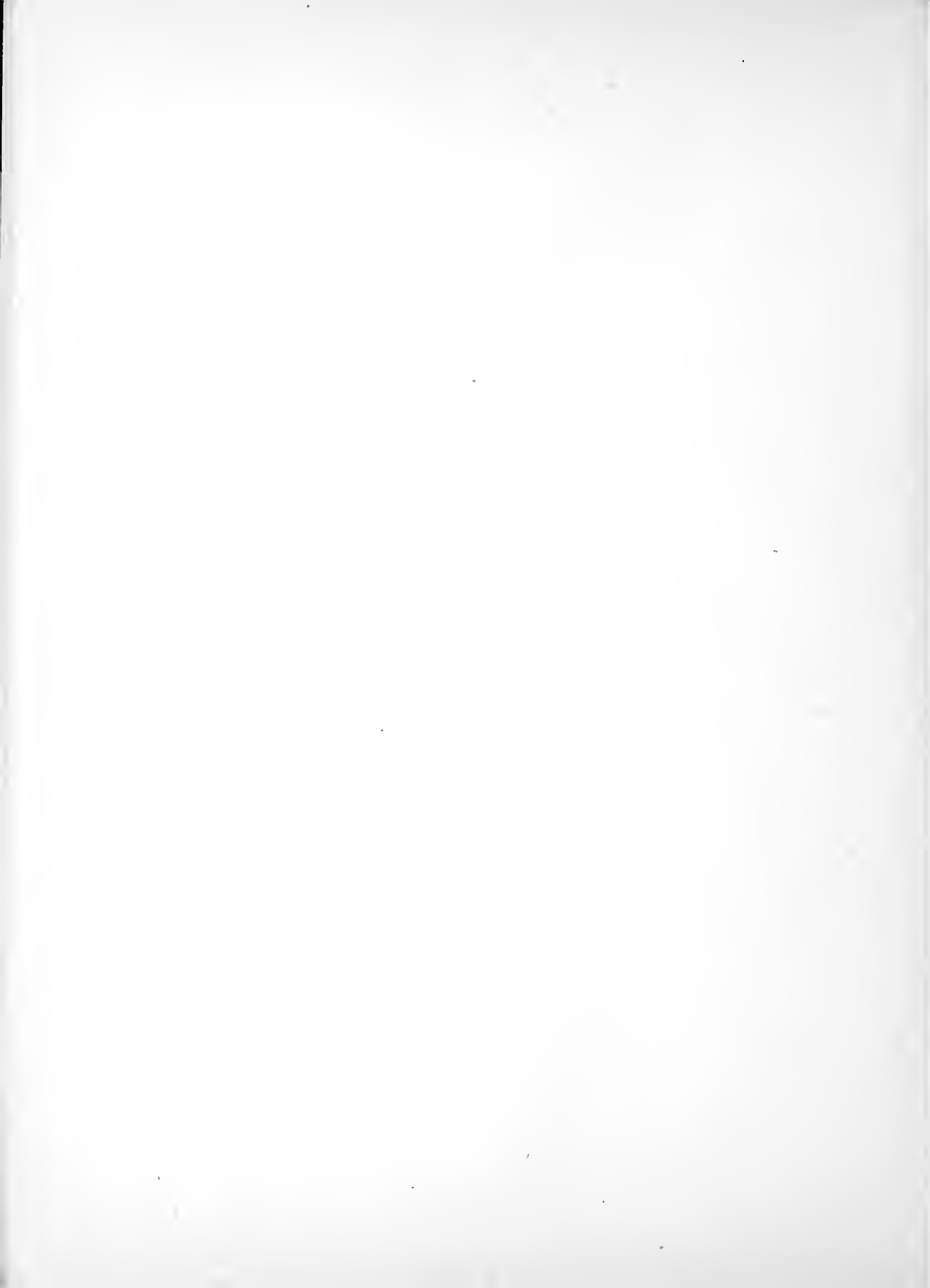


Figure 12.- Comparison of aileron effectiveness with partial-span flaps retracted and deflected. Aileron gaps sealed; $\alpha \approx 10^\circ$.



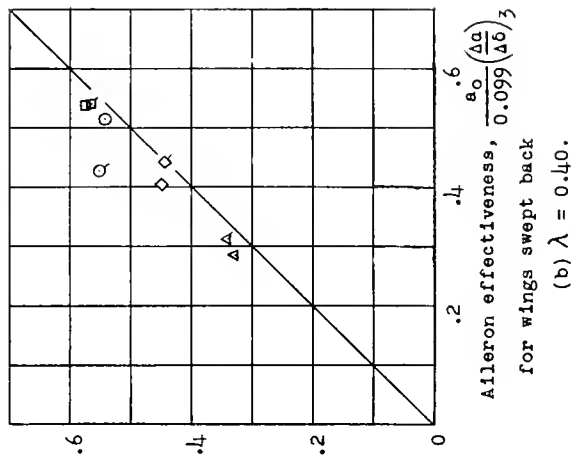
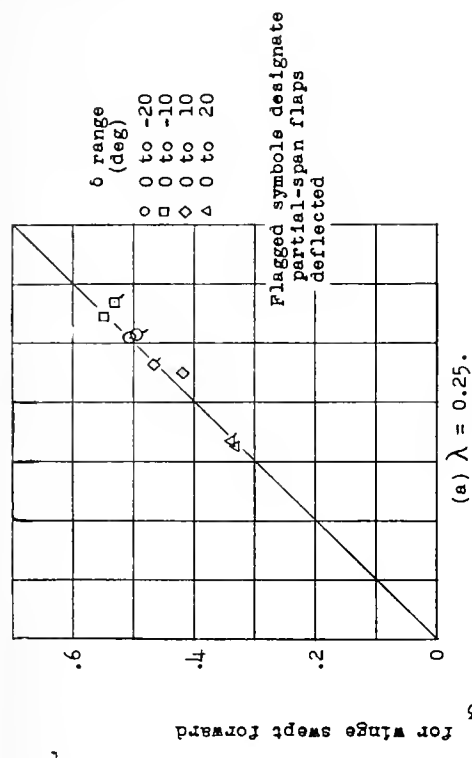


Figure 14.- Comparison of alleron effectiveness for wings with sweepback and sweepforward. Models 28 to 31; gaps sealed; $C_L = 0.8C_{L_{max}}$.

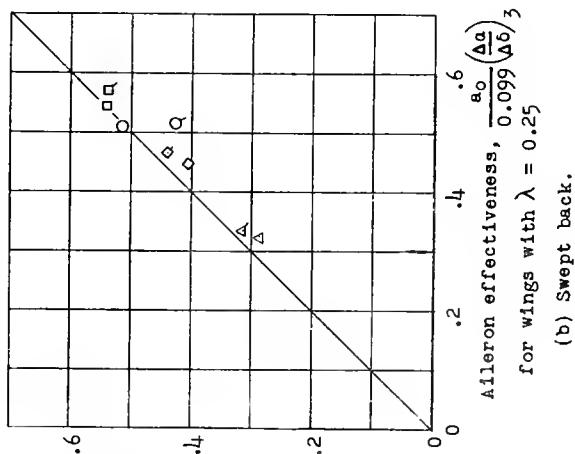
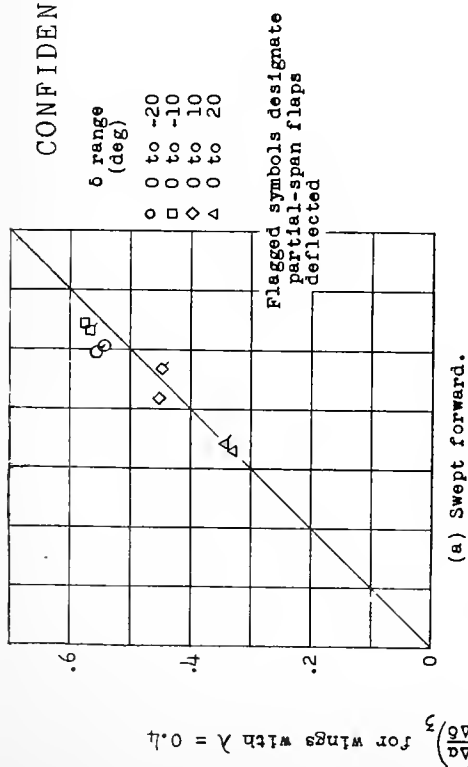
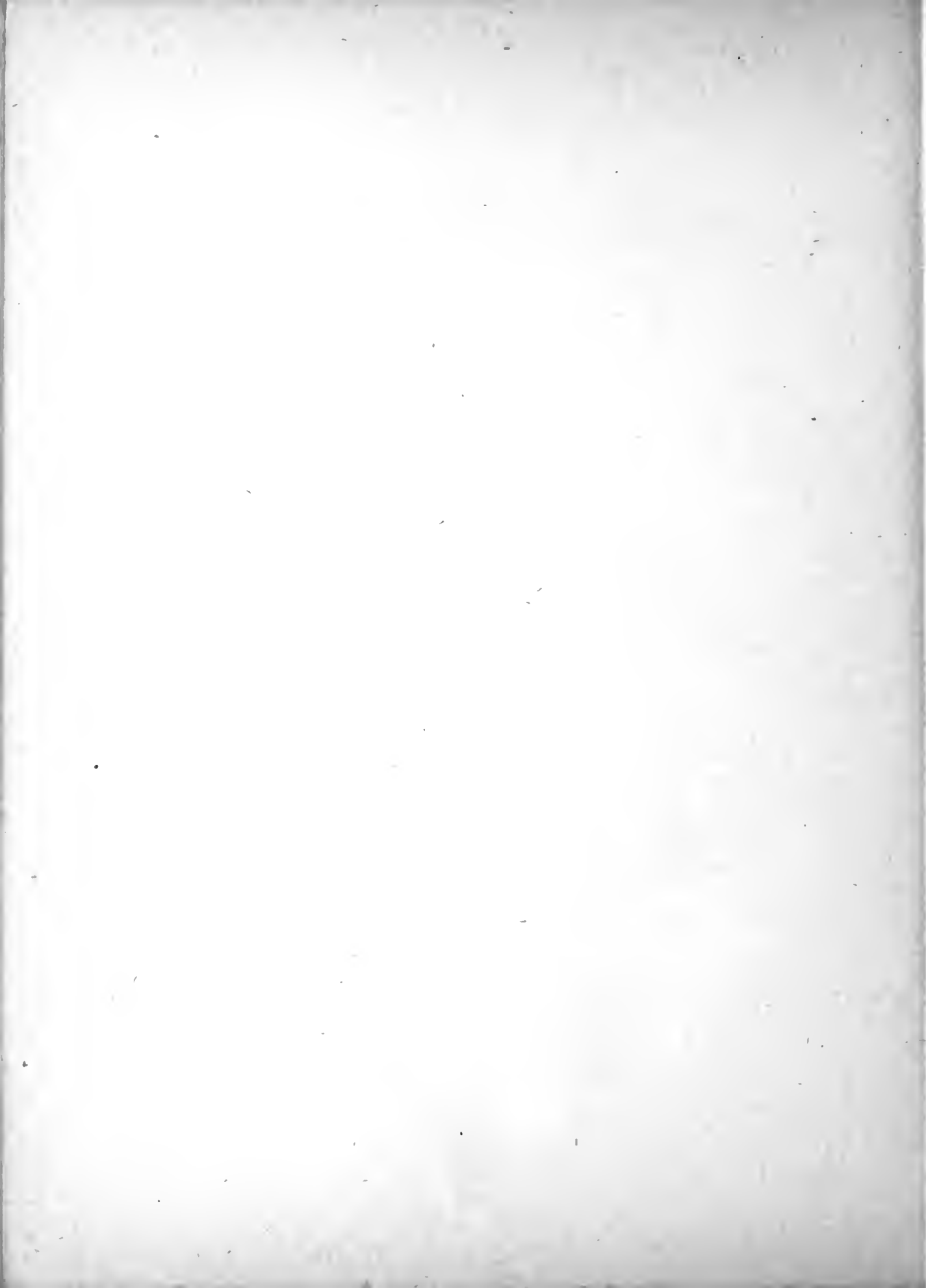


Figure 13.- Comparison of alleron effectiveness for wings with two amounts of taper. Models 28 to 31; gaps sealed; $C_L = 0.8C_{L_{max}}$.





UNIVERSITY OF FLORIDA



3 1262 08106 551 7